Basics of Tomography 2: Image Reconstruction

Prof. Dr. Marc Kachelrieß

German Cancer Research Center (DKFZ)
Heidelberg, Germany
www.dkfz.de/ct

DEUTSCHES
KREBSFORSCHUNGSZENTRUM
IN DER HELMHOLTZ-GEMEINSCHAFT

Fan-Beam Geometry (transaxial / in-plane / x-y-plane)

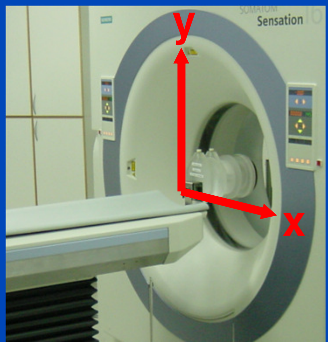

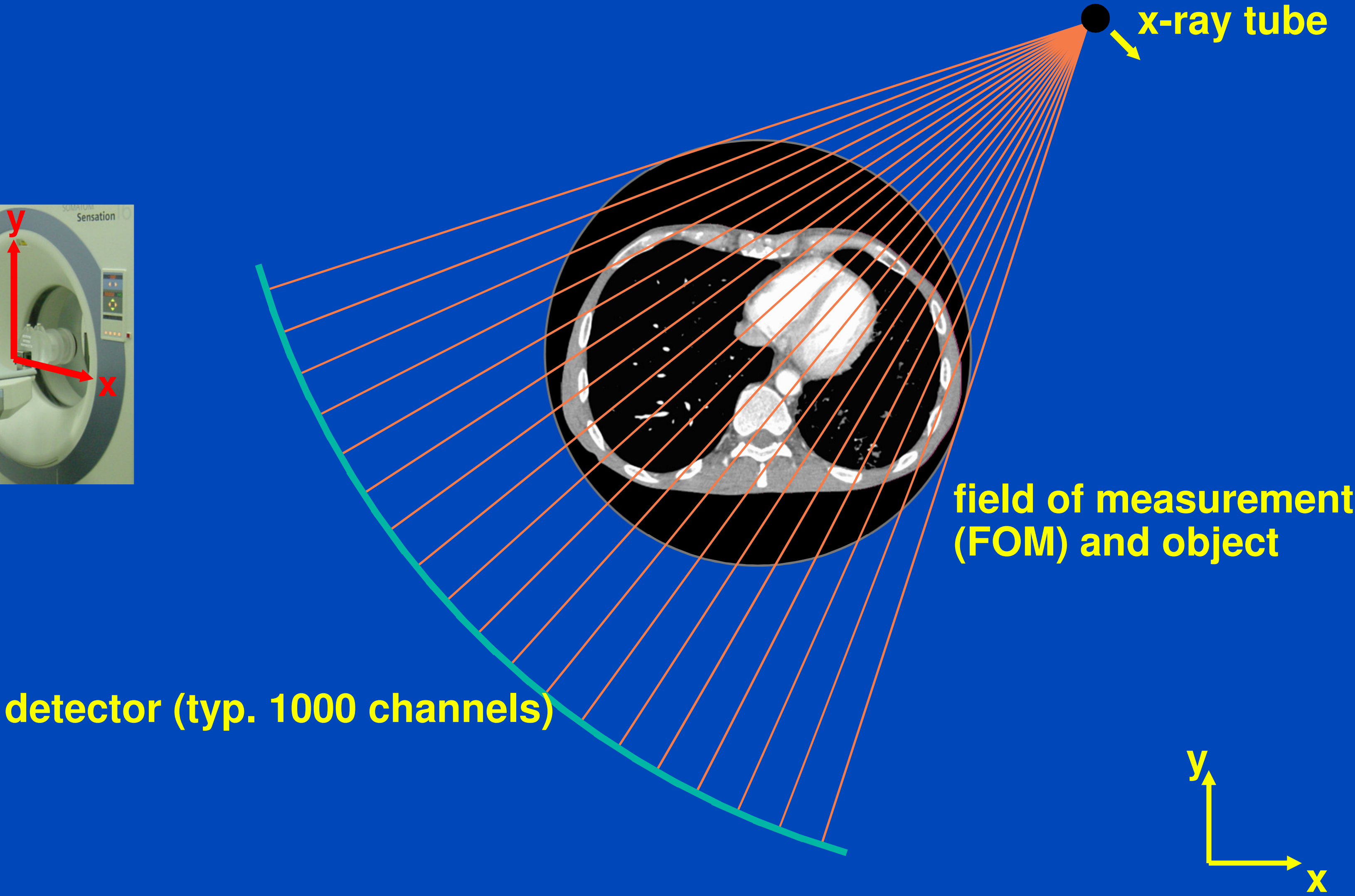

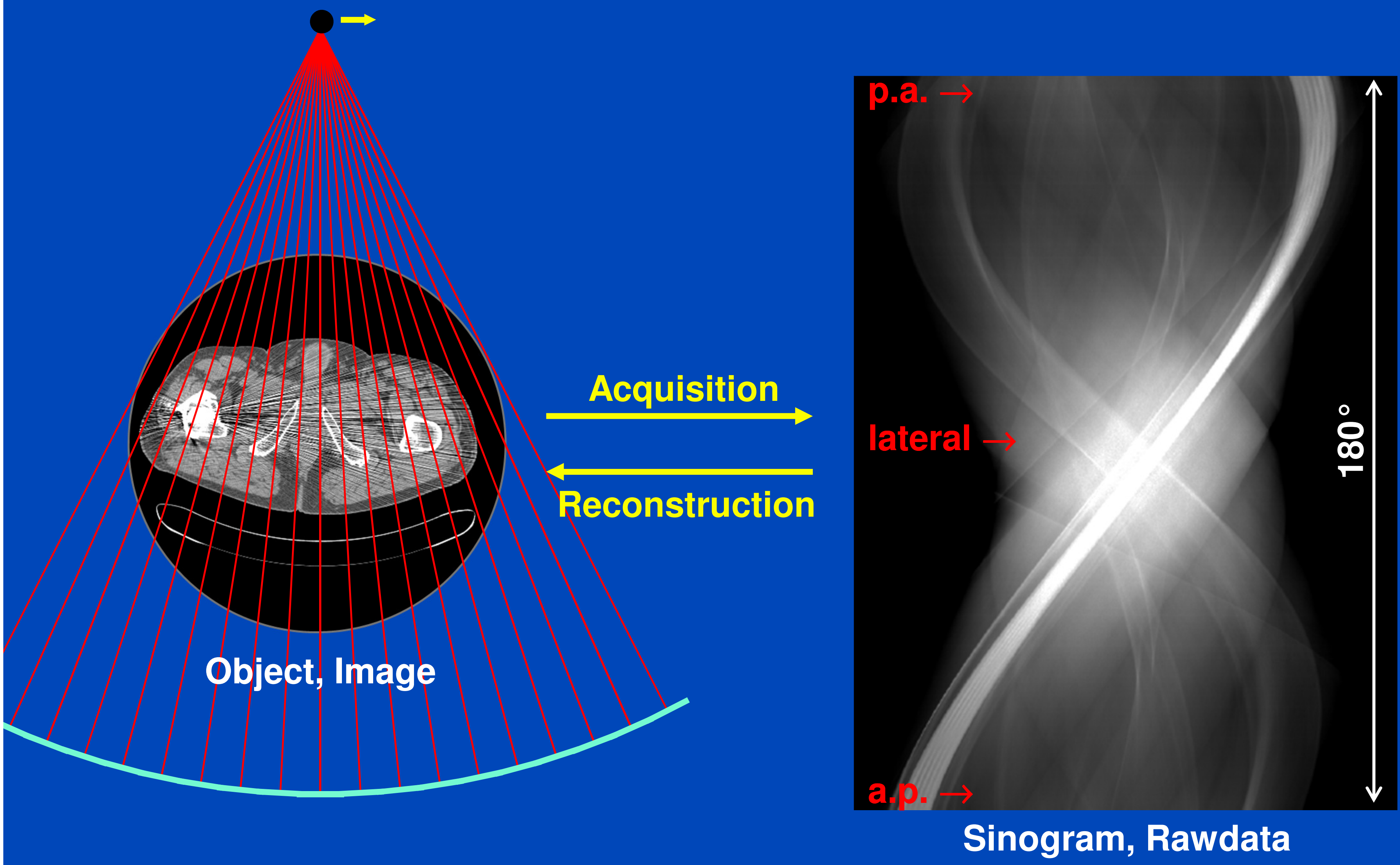

Acquisition
Reconstruction
Object, Image
p.a. →
lateral →
a.p. →
180°
Sinogram, Rawdata

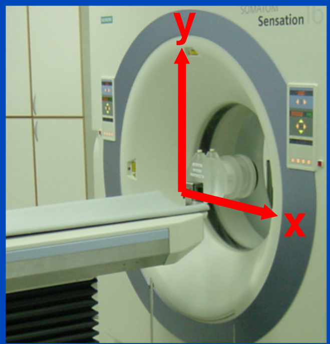

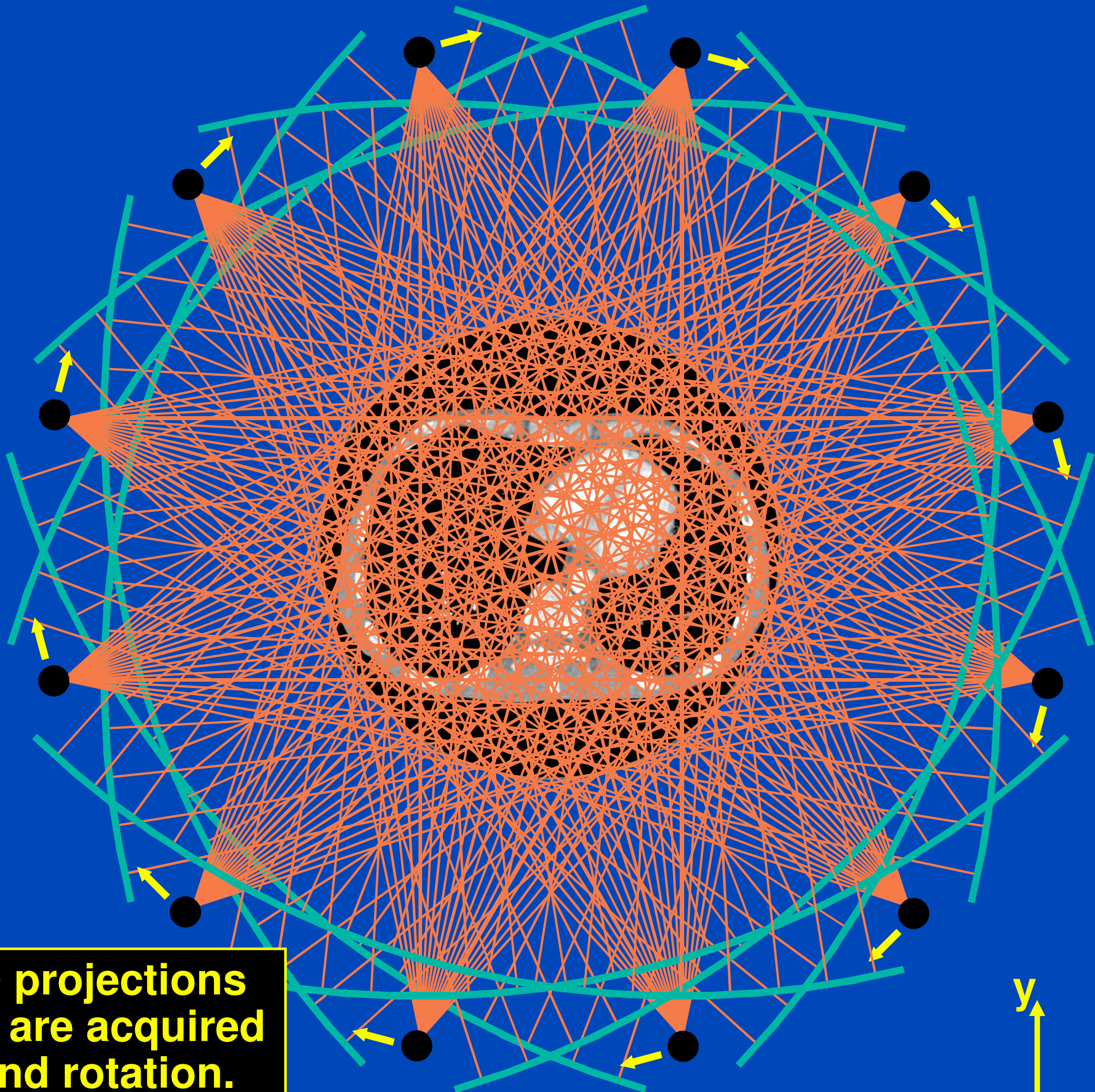

In the order of 1000 projections with 1000 channels are acquired per detector slice and rotation.

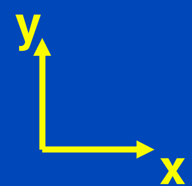

Data Completeness

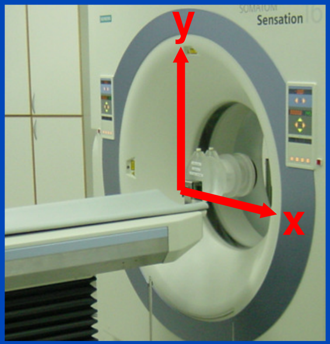

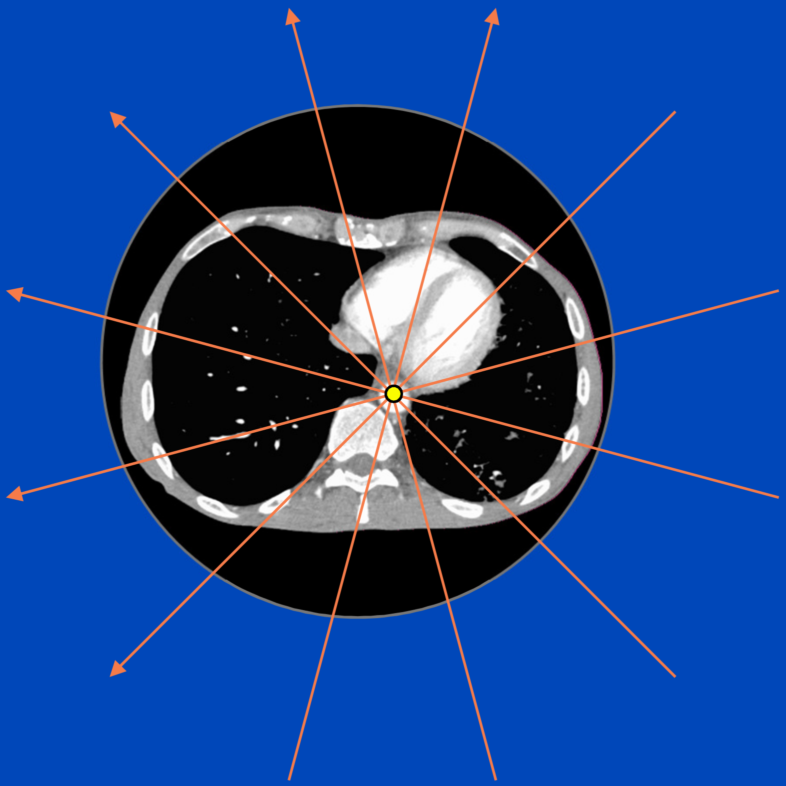

Each object point must be viewed by an angular interval of 180° or more. Otherwise image reconstruction is not possible.

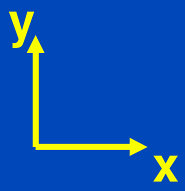

Emission vs. Transmission

Emission tomography

- Infinitely many sources
- No source trajectory
- Detector trajectory may be an issue
- 3D reconstruction relatively simple

Transmission tomography

- A single source
- Source trajectory is the major issue
- Detector trajectory is an important issue
- 3D reconstruction extremely difficult

Analytical Image Reconstruction

$$x^2 = y$$

Model

$$x = \sqrt{y}$$

Solution

2D: In-Plane Geometry

- Decouples from longitudinal geometry
- Useful for many imaging tasks
- Easy to understand
- 2D reconstruction
  - Rebinning = resampling, resorting
  - Filtered backprojection

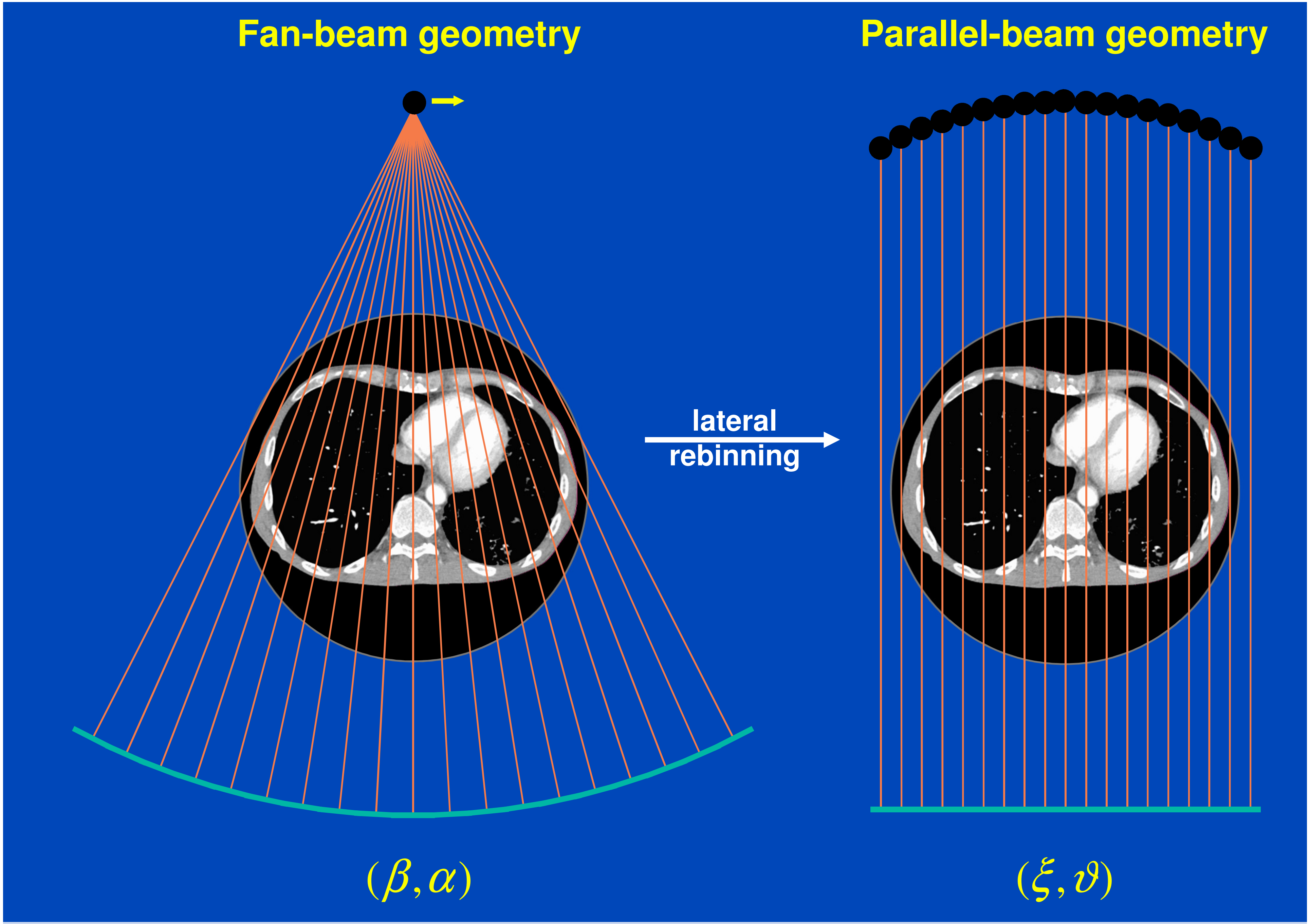
Fan-beam geometry
Parallel-beam geometry
lateral
rebinning
(β, α)
(ξ, ϑ)

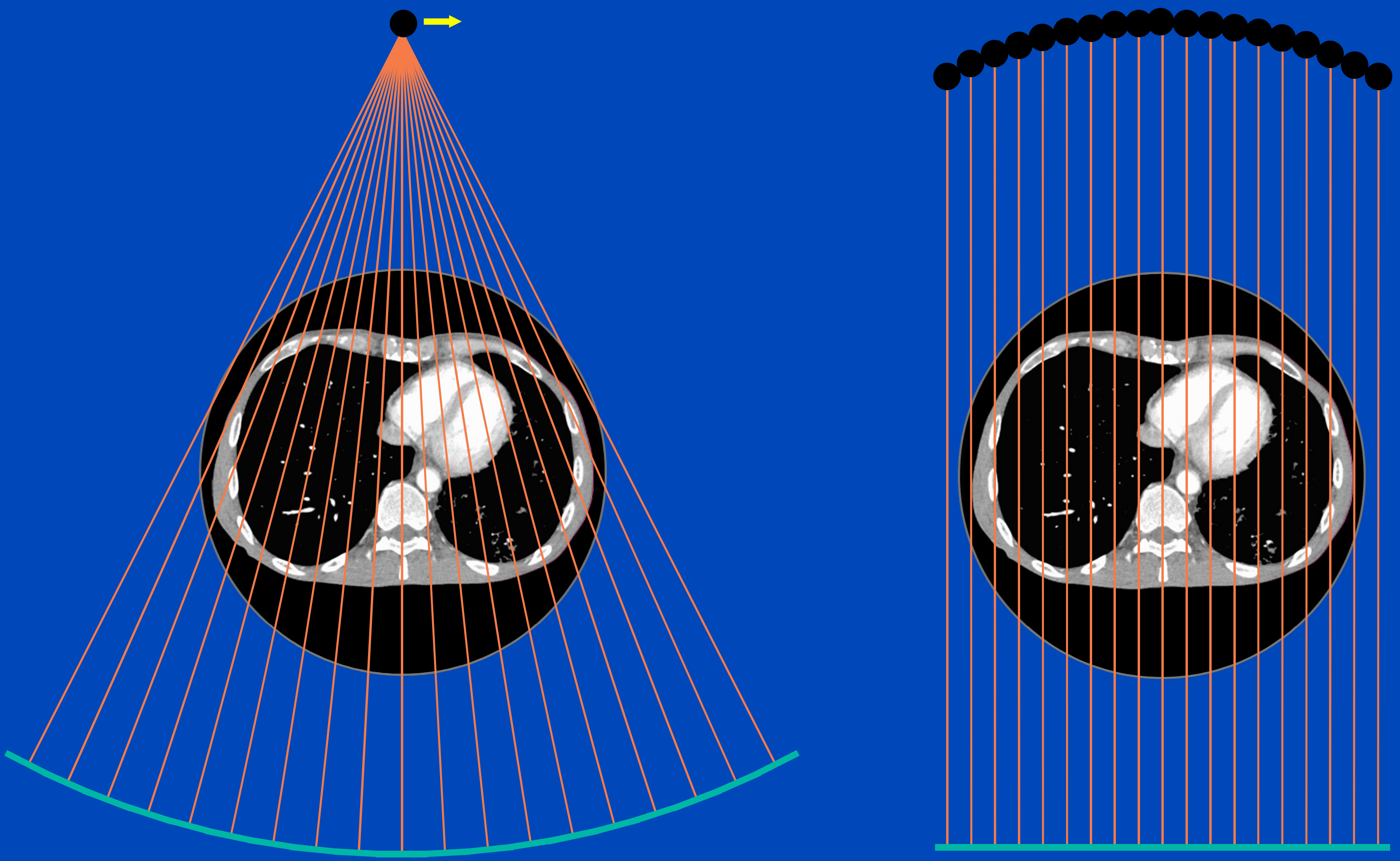

Fan-beam geometry

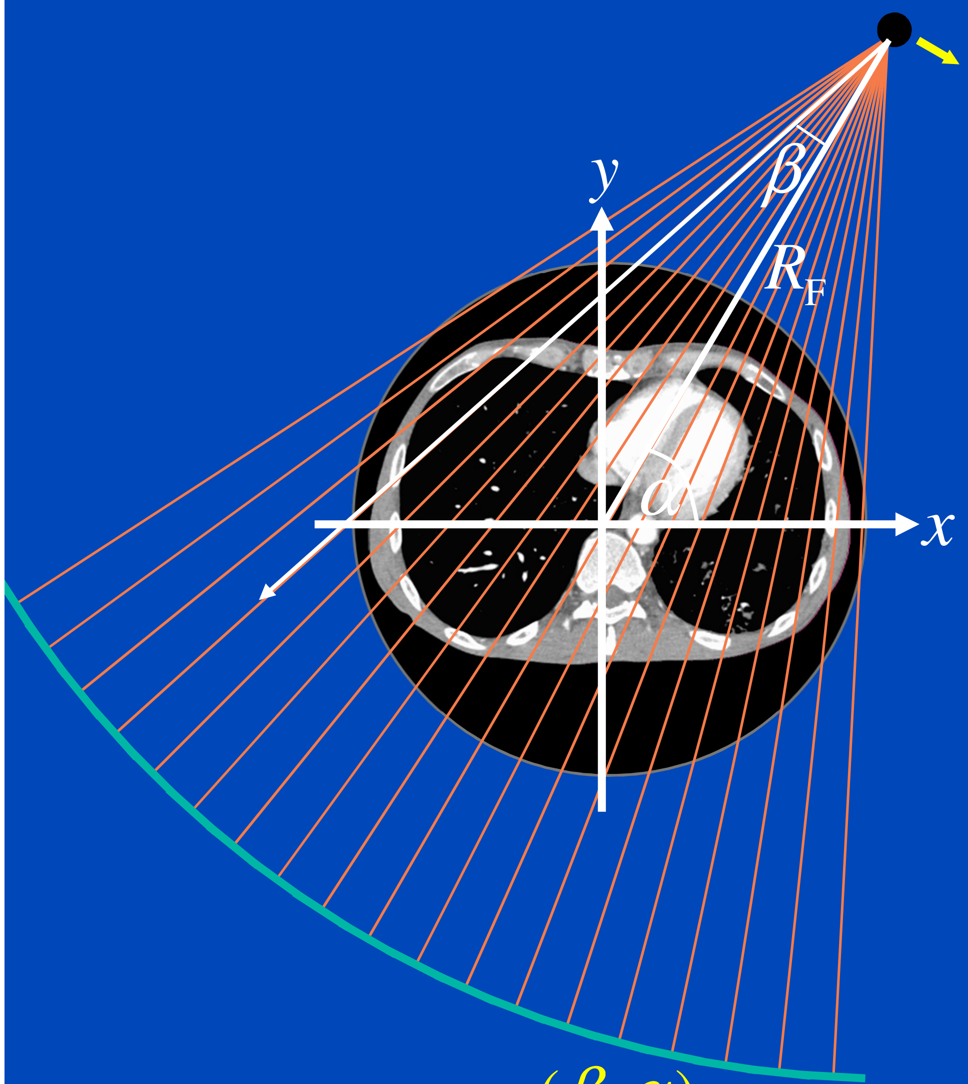

(β, α)

Parallel-beam geometry

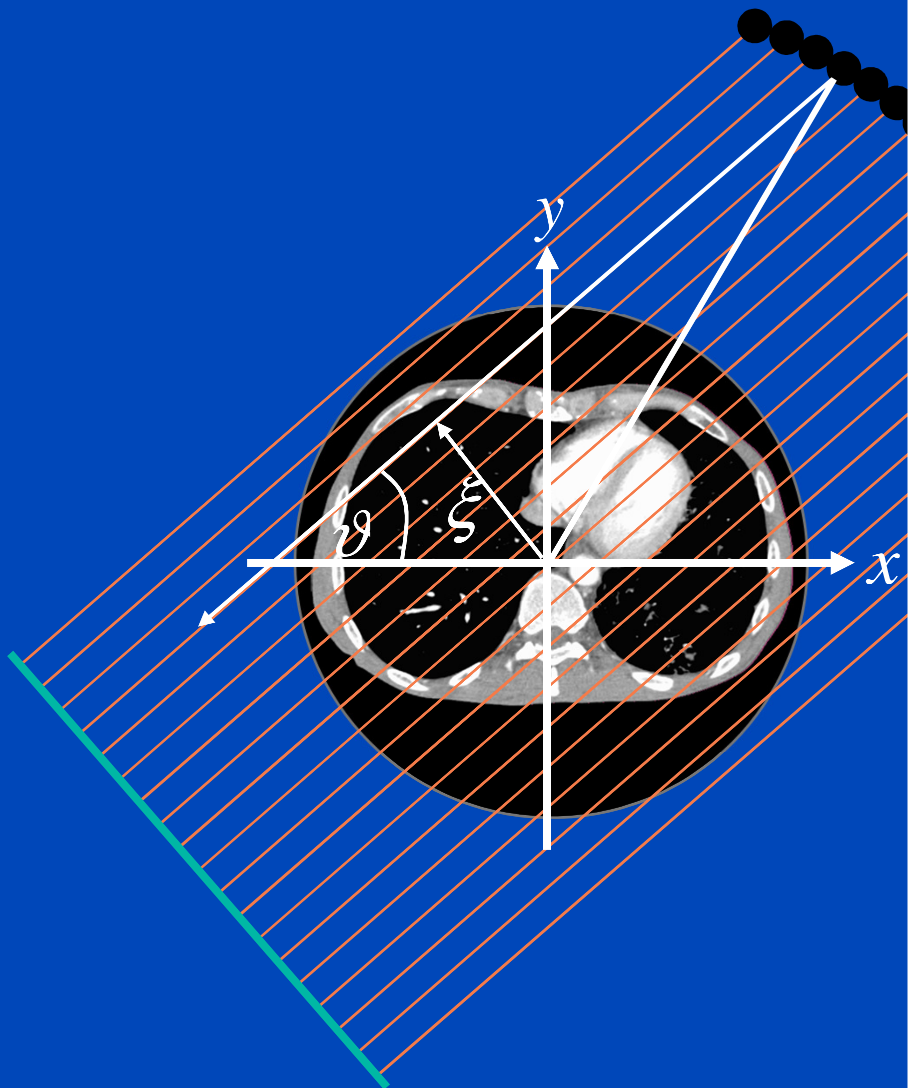

(ξ, ϑ)

In-Plane Parallel Beam Geometry

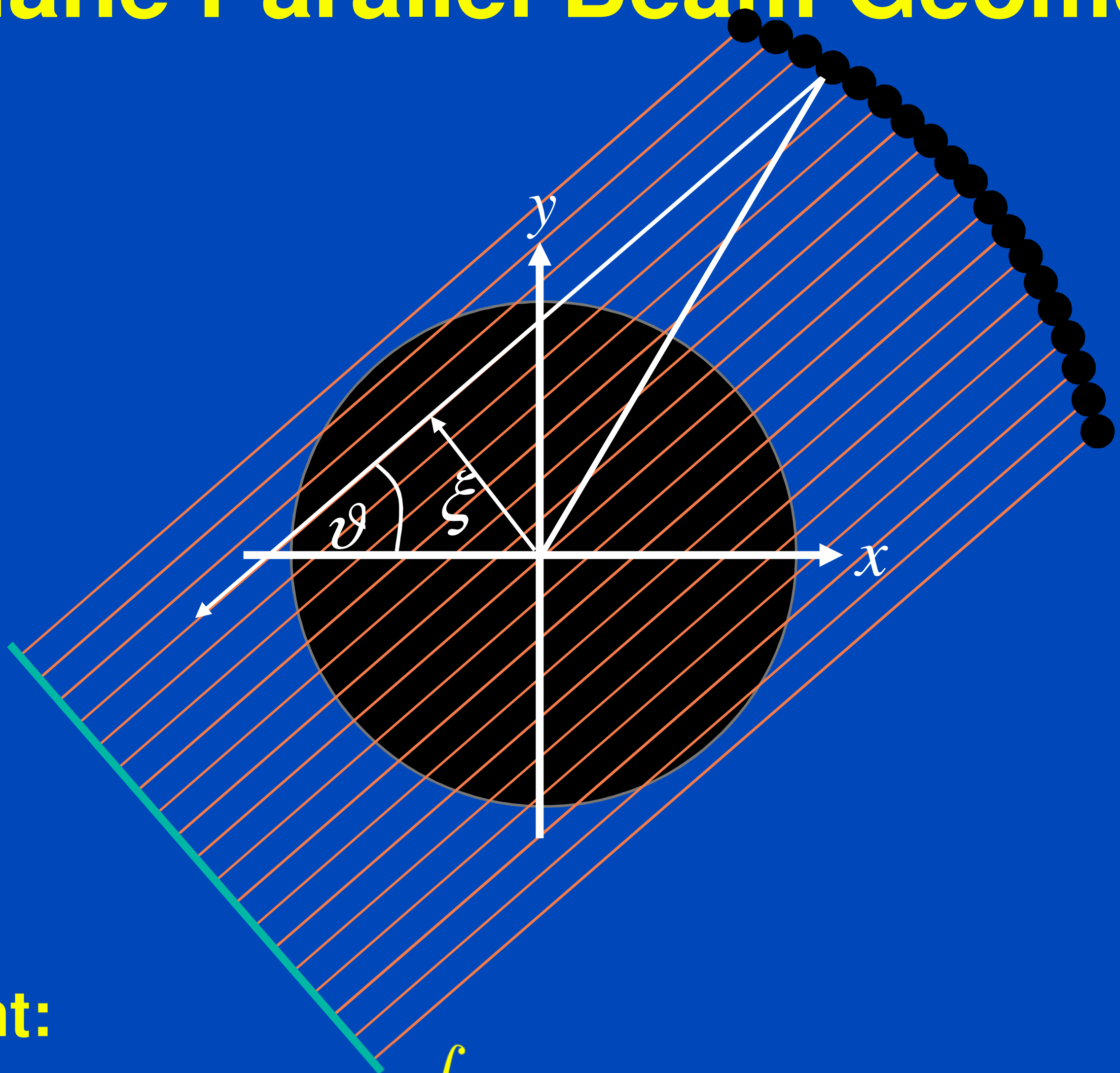

Measurement:

$$p(\vartheta,\xi) = \mathsf{R}f(\vartheta,\xi) = \int dx\,dy\; f(x,y)\,\delta(x\cos\vartheta + y\sin\vartheta - \xi)$$

Filtered Backprojection (FBP)

Measurement: $p(\vartheta,\xi) = \int dxdy\, f(x,y)\delta(x\cos\vartheta + y\sin\vartheta - \xi)$

Fourier transform:

$$\int d\xi\, p(\vartheta,\xi)e^{-2\pi i\xi u} = \int dxdy\, f(x,y)e^{-2\pi iu(x\cos\vartheta + y\sin\vartheta)}$$

This is the central slice theorem: $P(\vartheta,u) = F(u\cos\vartheta, u\sin\vartheta)$

Inversion: $f(x,y) = \int\limits_0^\pi d\vartheta \int\limits_{-\infty}^{\infty} du\, |u| P(\vartheta,u)e^{2\pi iu(x\cos\vartheta + y\sin\vartheta)}$

$$= \int\limits_0^\pi d\vartheta\, p(\vartheta,\xi) * k(\xi)\Big|_{\xi = x\cos\vartheta + y\sin\vartheta}$$

dkfz.

Filtered Backprojection (FBP)

1. Filter projection data with the reconstruction kernel.
2. Backproject the filtered data into the image:

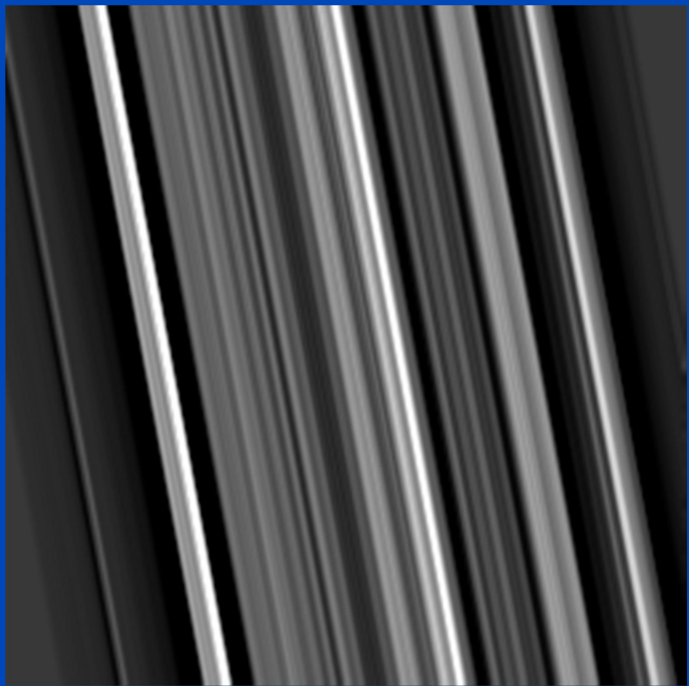

Smooth

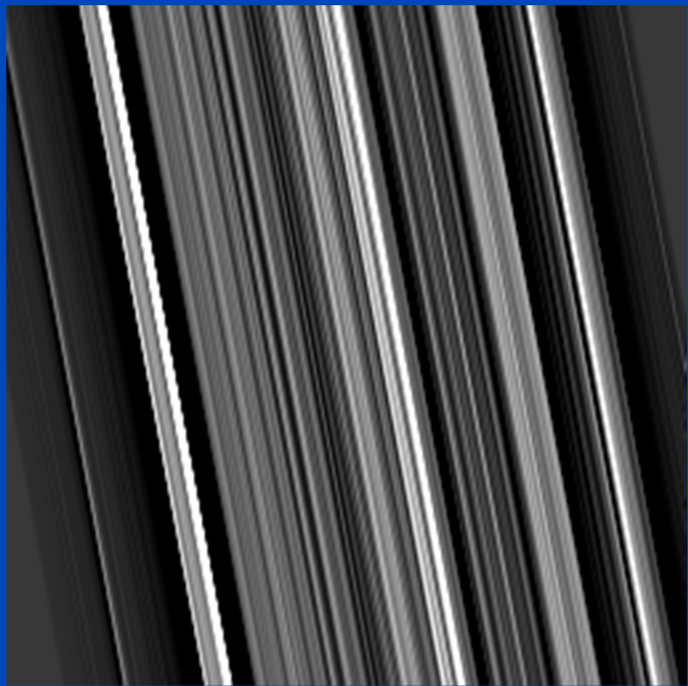

Standard

Reconstruction kernels balance between spatial resolution and image noise.

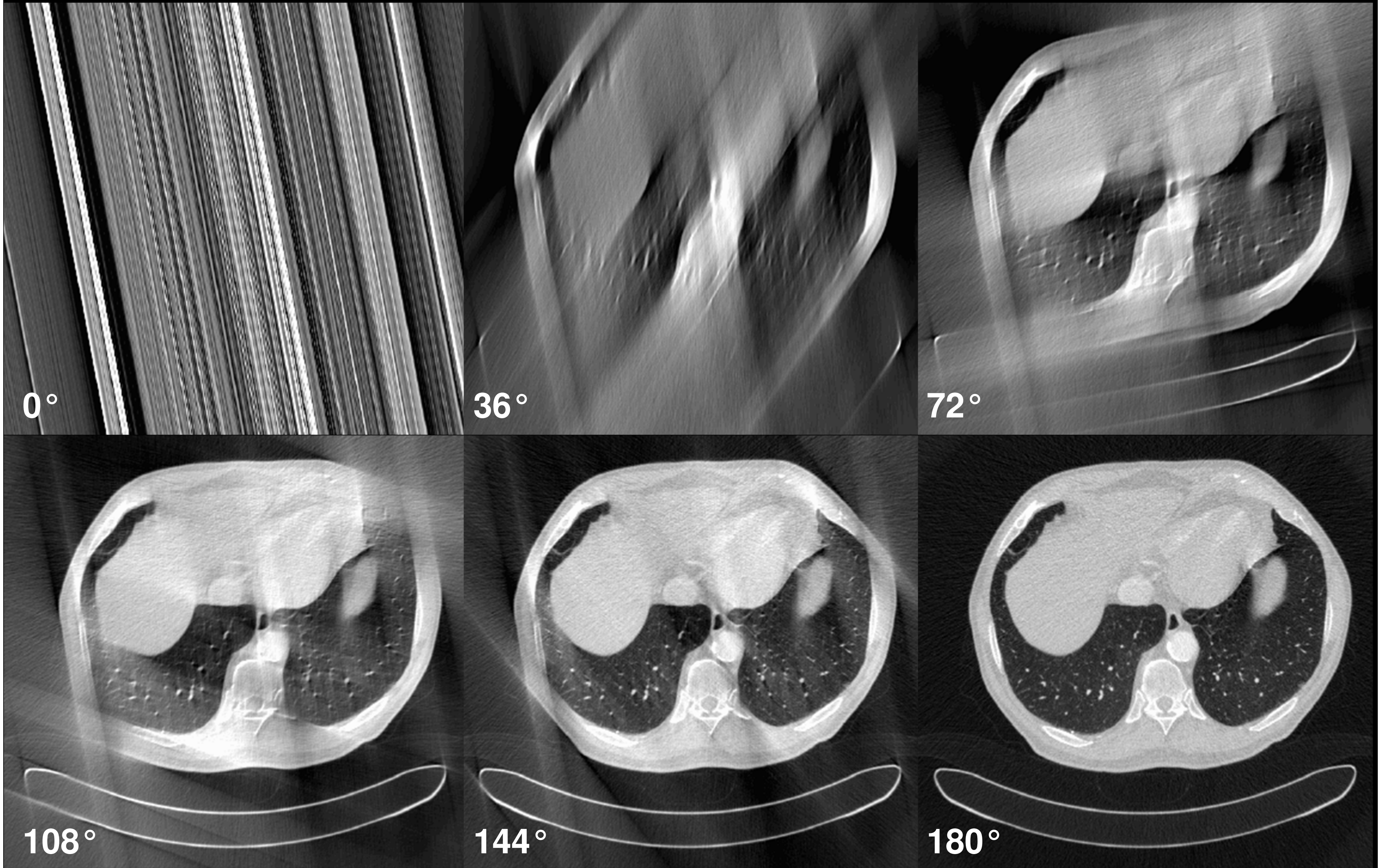
0°
36°
72°
108°
144°
180°

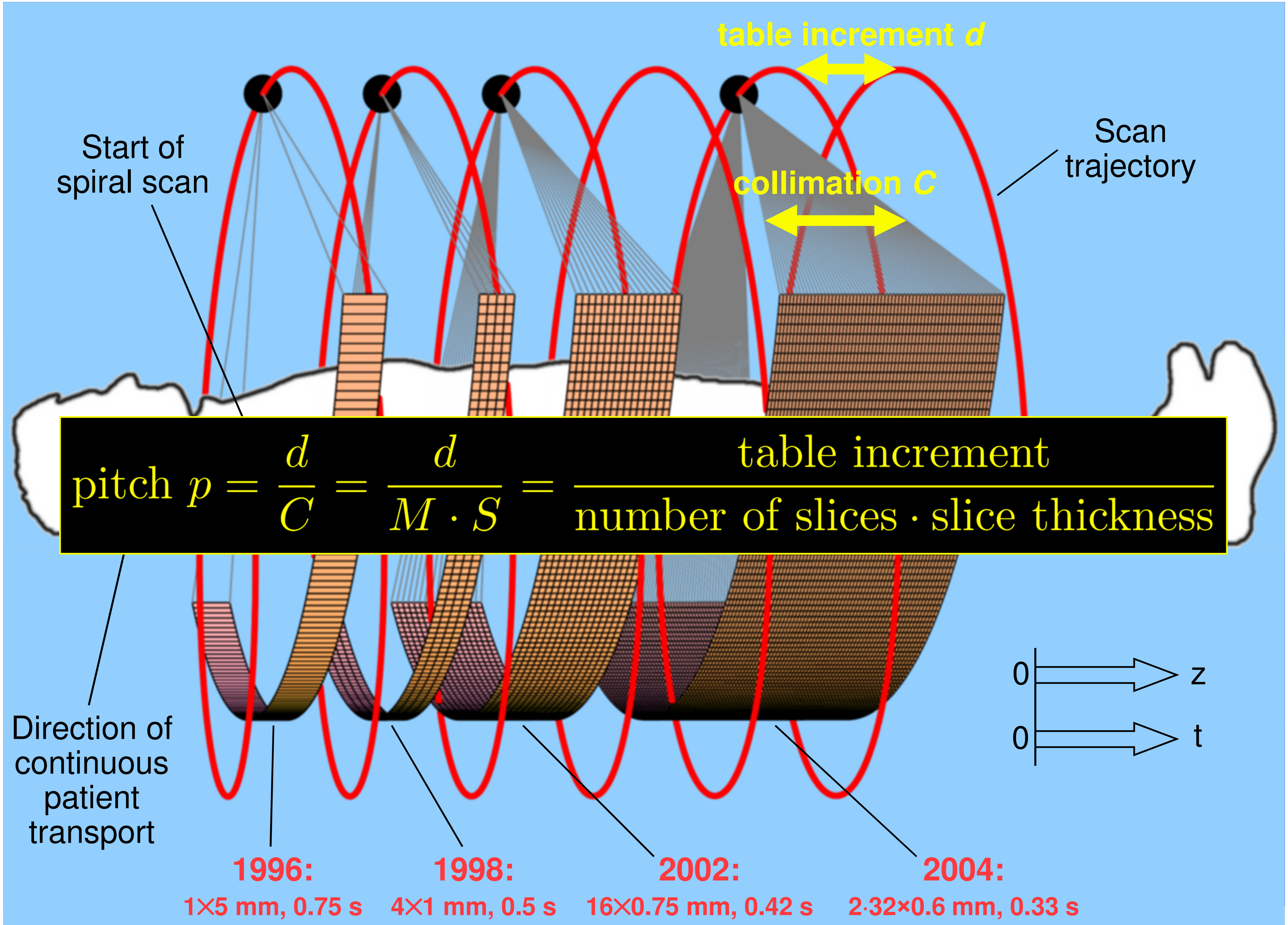

$$\text{pitch } p = \frac{d}{C} = \frac{d}{M \cdot S} = \frac{\text{table increment}}{\text{number of slices} \cdot \text{slice thickness}}$$

Kalender et al., Radiology 173(P):414 (1989) and 176:181-183 (1990)

360° LI Spiral z-Interpolation for Single-Slice CT (M=1)

$$p = \frac{d}{MS} \leq 2$$

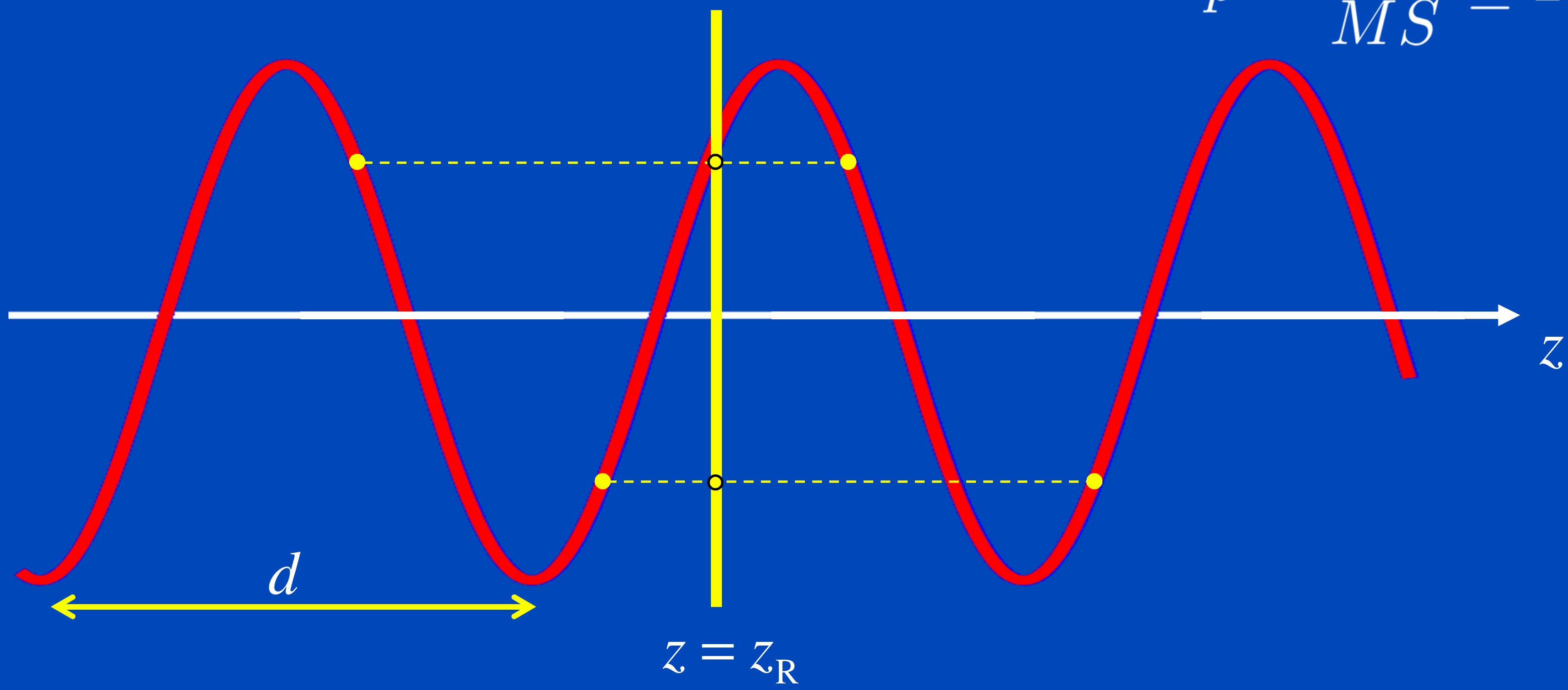

Spiral z-interpolation is typically a linear interpolation between points adjacent to the reconstruction position to obtain circular scan data.

without *z*-interpolation

with *z*-interpolation

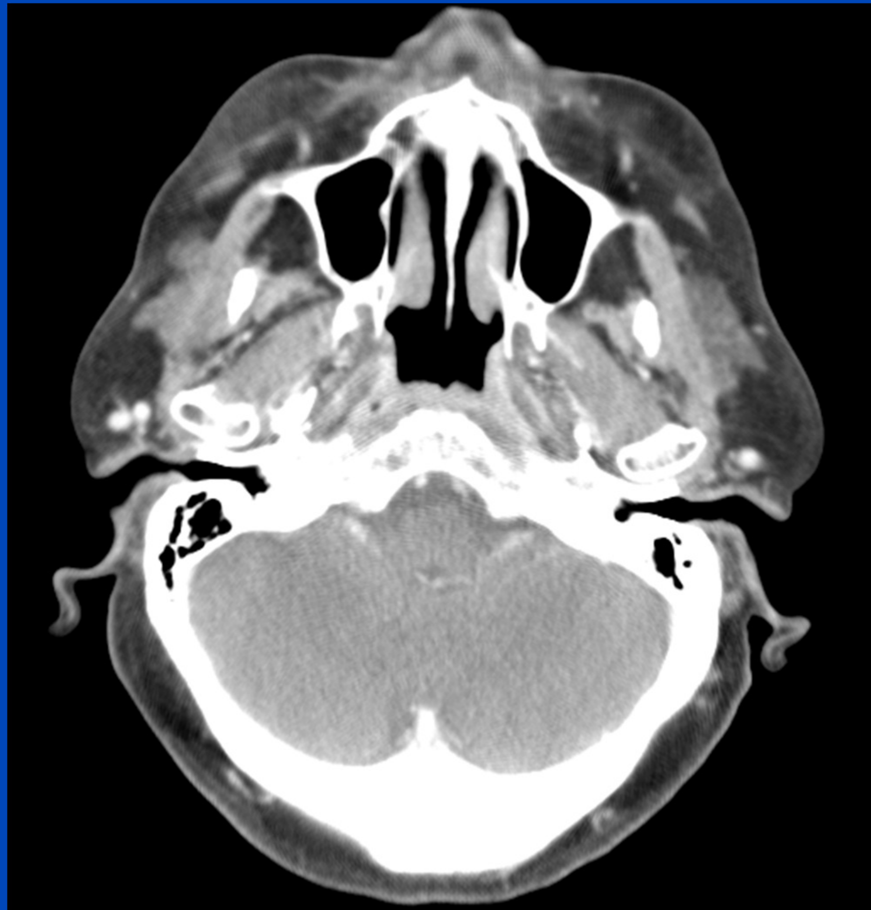

180° LI Spiral z-Interpolation for Single-Slice CT (*M*=1)

$$p = \frac{d}{MS} \leq 2$$

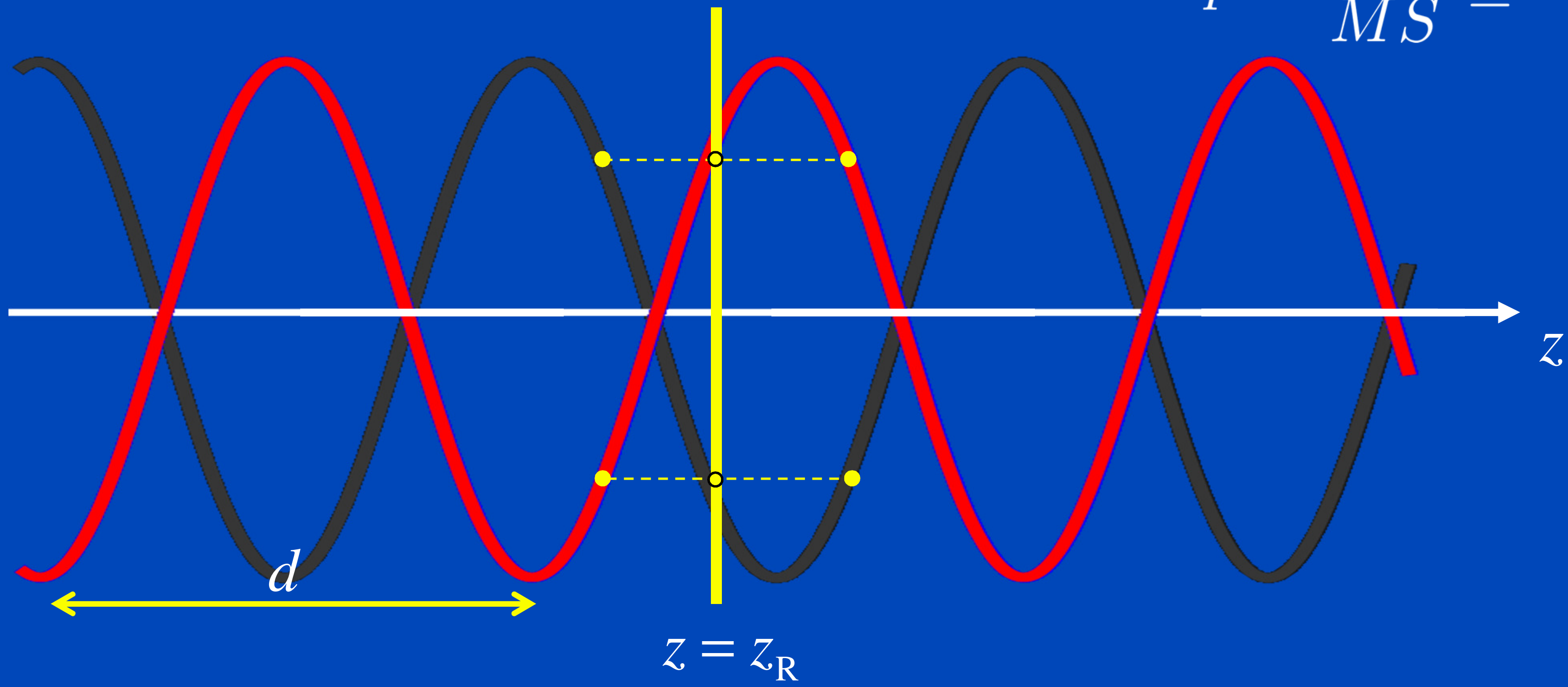

180° Spiral z-interpolation interpolates between direct and complementary rays.

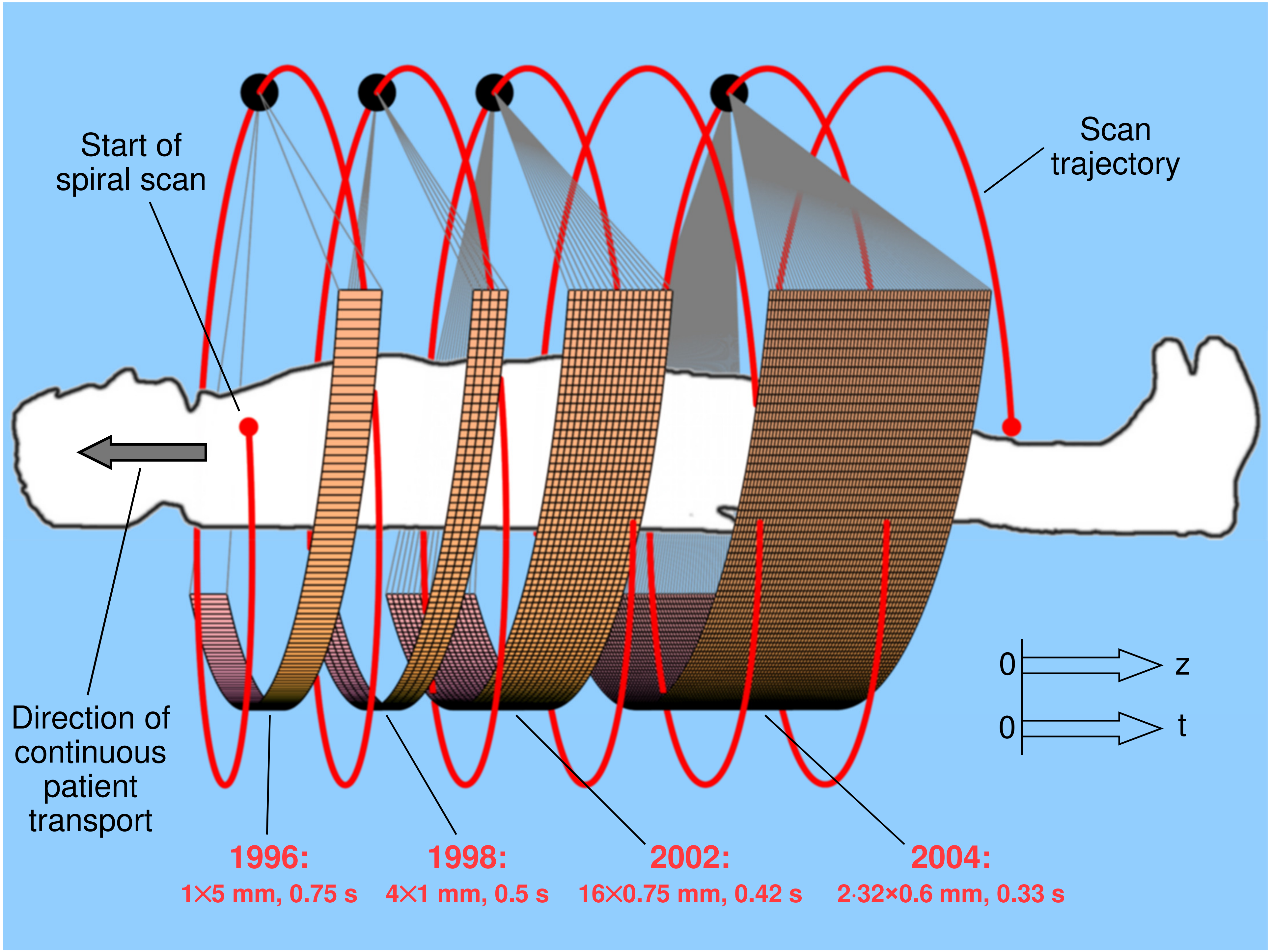
Start of
spiral scan
Scan
trajectory
Direction of
continuous
patient
transport
0
z
0
t
1996:
1×5 mm, 0.75 s
1998:
4×1 mm, 0.5 s
2002:
16×0.75 mm, 0.42 s
2004:
2·32×0.6 mm, 0.33 s

Spiral z-Filtering for Multi-Slice CT
M=2, …, 6

$$p = \frac{d}{MS} \leq 1.5$$

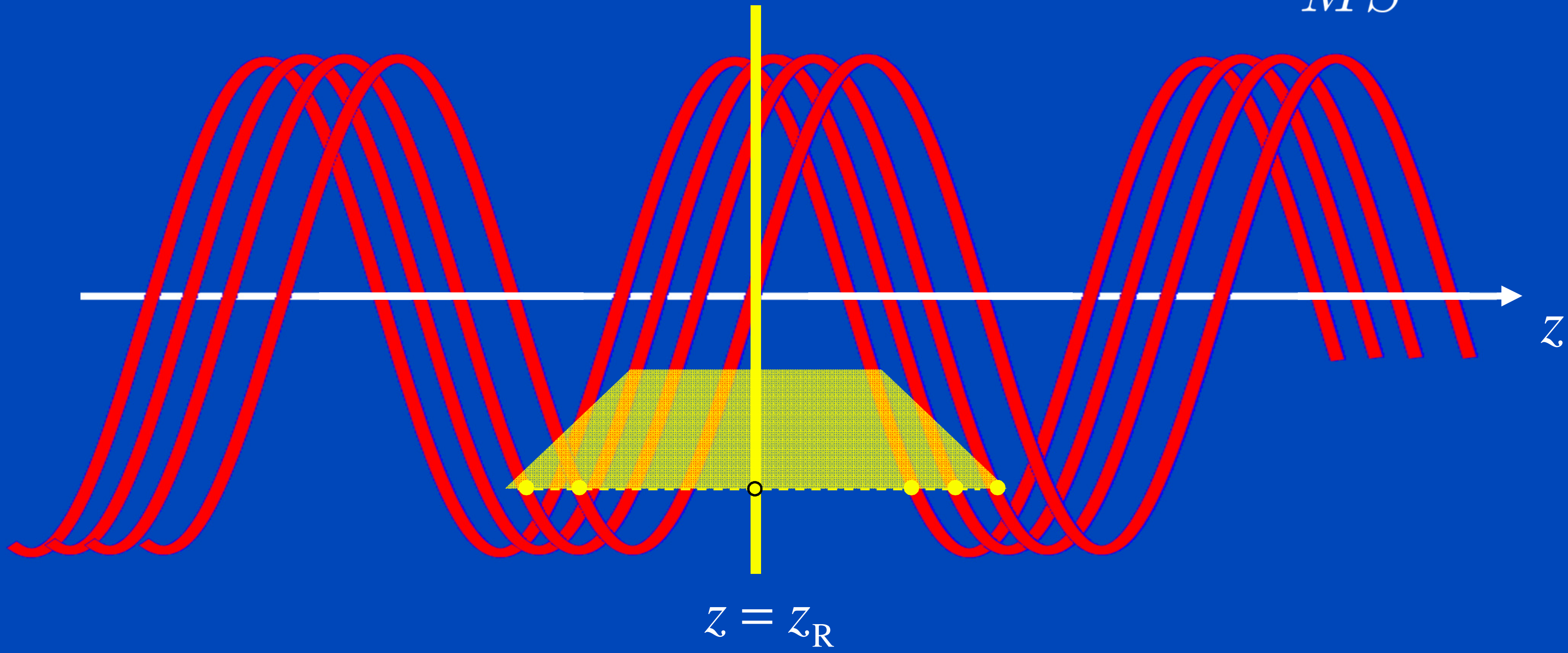

Spiral z-filtering is collecting data points weighted with a triangular or trapezoidal distance weight to obtain circular scan data.

dkfz.

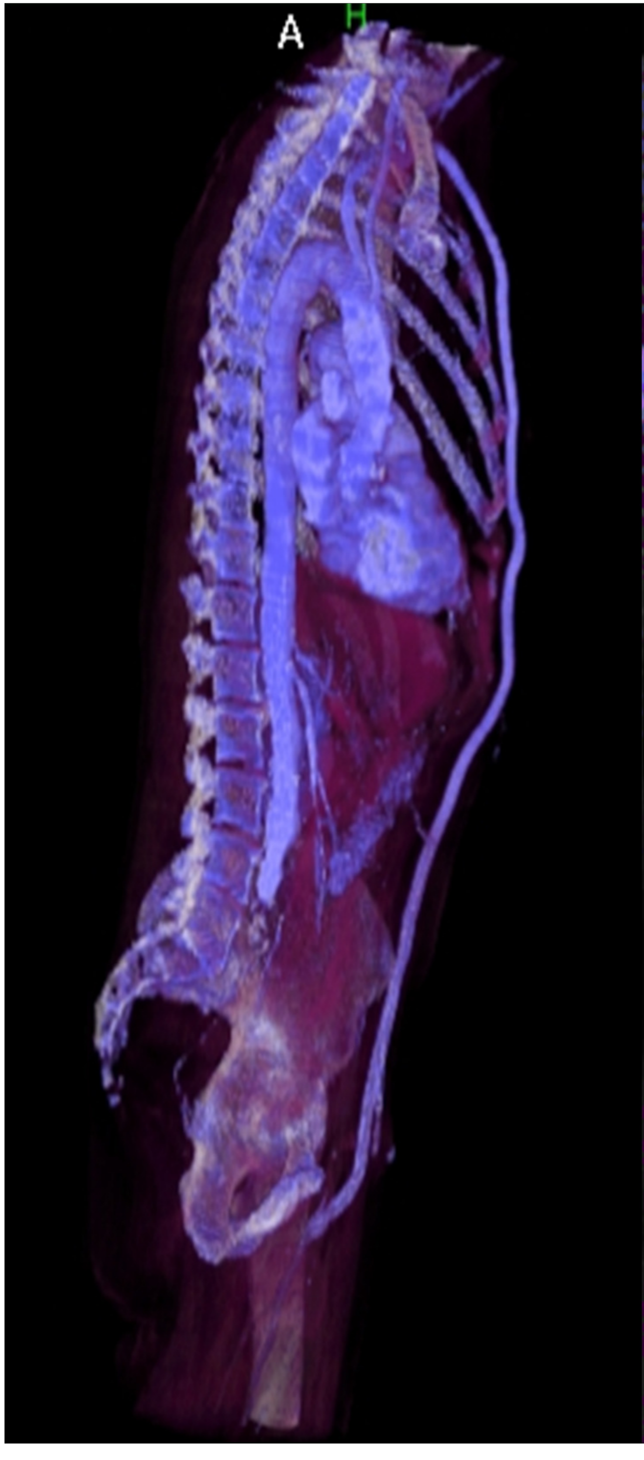

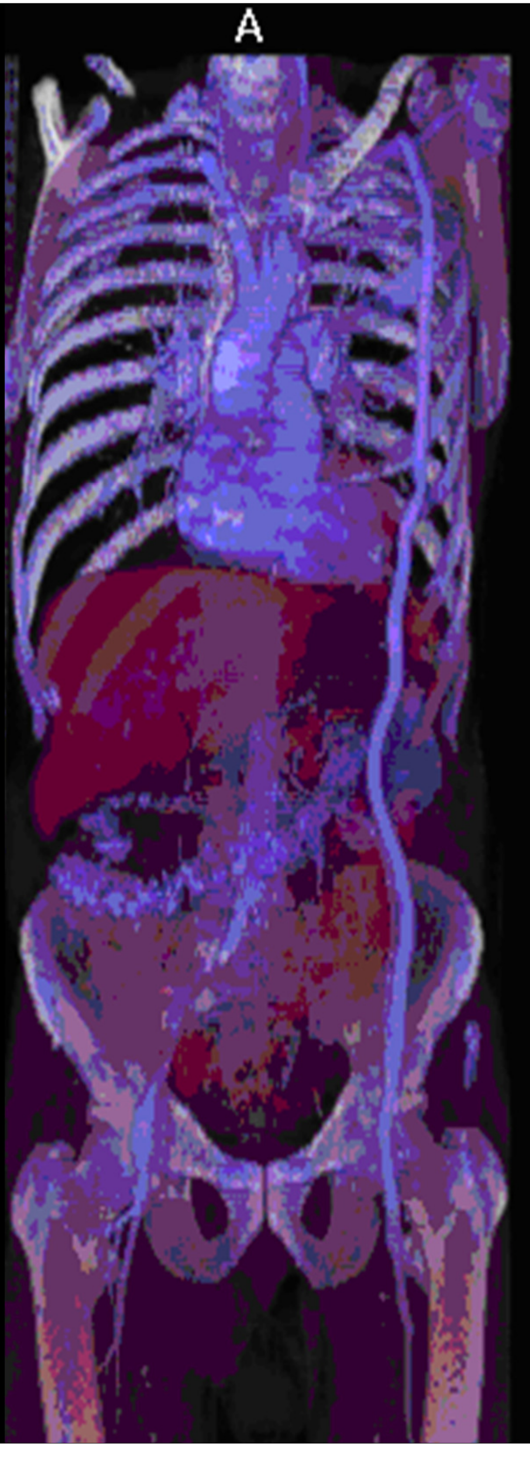

CT Angiography: Axillo-femoral bypass

$M = 4$

120 cm in 40 s

0.5 s per rotation
4×2.5 mm collimation
pitch 1.5

RSNA 1989
SSCT (*M* = 1)

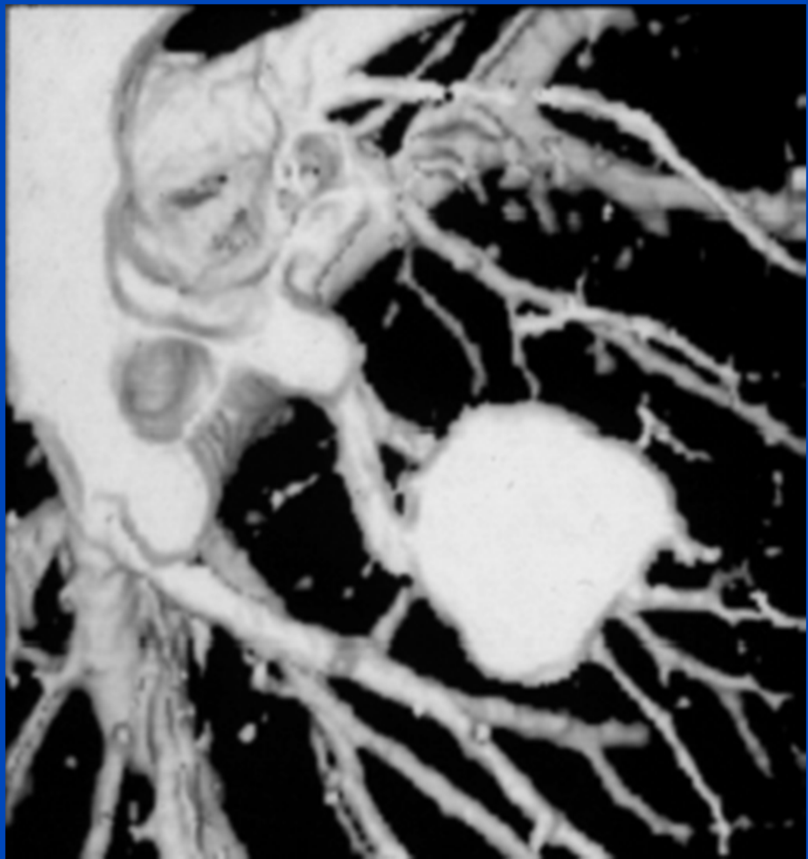

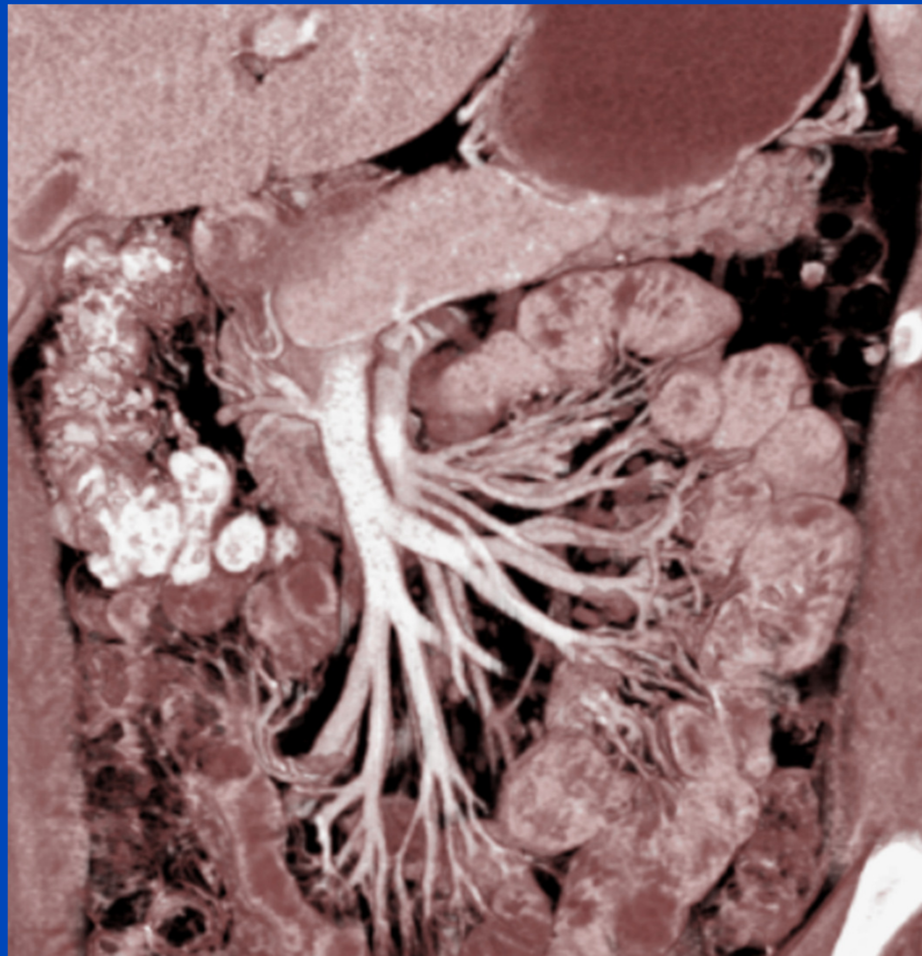

RSNA 2001
MSCT (*M* = 16)

dkfz.

The Pitch Value is the Measure for Scan Overlap

The pitch is defined as the ratio of the table increment per full rotation to the *total* collimation width in the center of rotation:

$$p = \frac{d}{C} = \frac{d}{MS}$$

Recommended by and in:

IEC, International Electrotechnical Commision: Medical electrical equipment – 60601 Part 2-44: Particular requirements for the safety of x-ray equipment for computed tomography. Geneva, Switzerland, 1999.

Examples:

- p=1/3=0.333 means that each z-position is covered by 3 rotations (3-fold overlap)
- p=1 means that the acquisition is not overlapping
- $p=p_{max}$ means that each z-position is covered by half a rotation

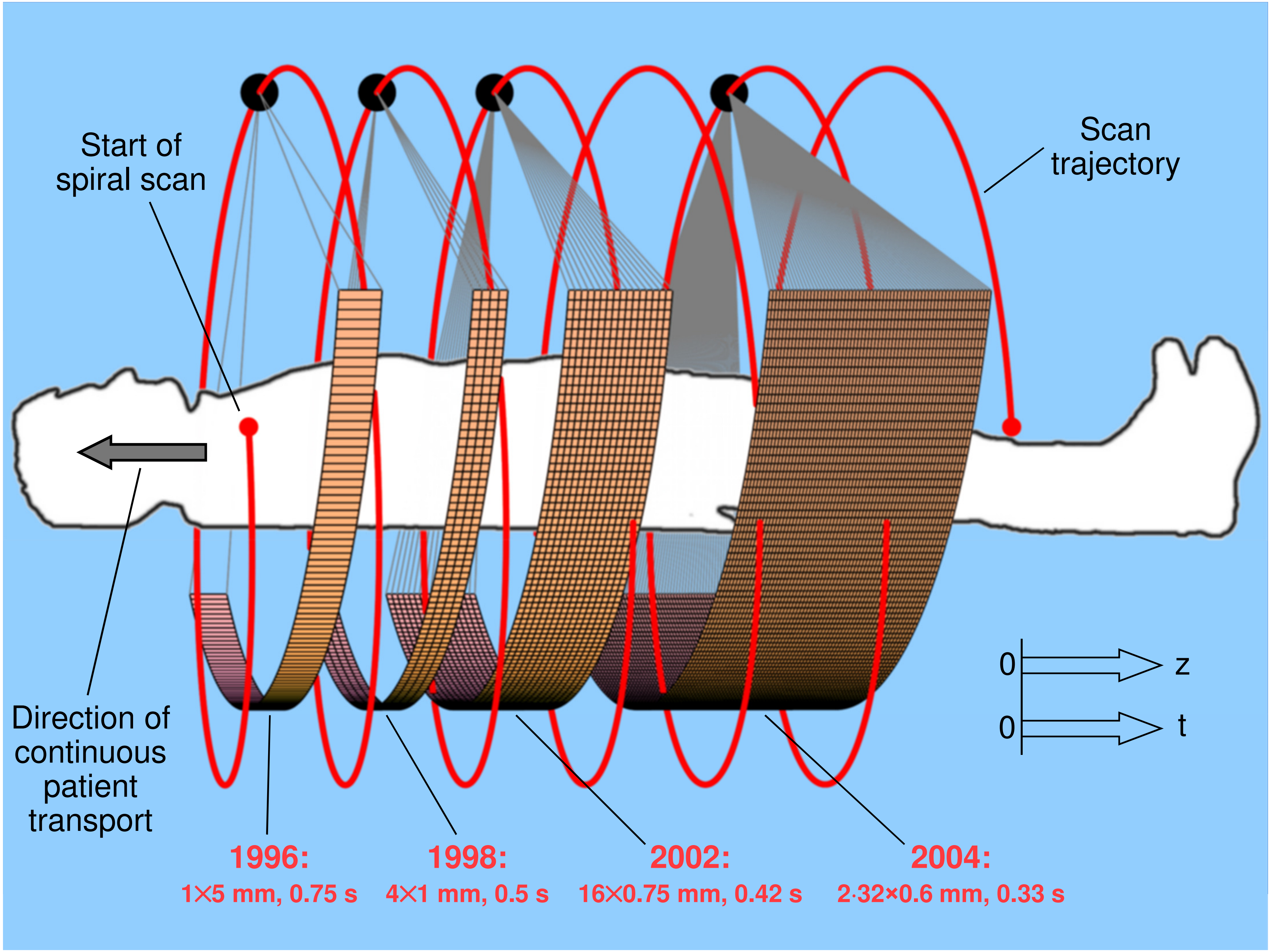
Start of spiral scan
Scan trajectory
Direction of continuous patient transport
0 z
0 t
1996:
1×5 mm, 0.75 s
1998:
4×1 mm, 0.5 s
2002:
16×0.75 mm, 0.42 s
2004:
2·32×0.6 mm, 0.33 s

The Cone-Beam Problem

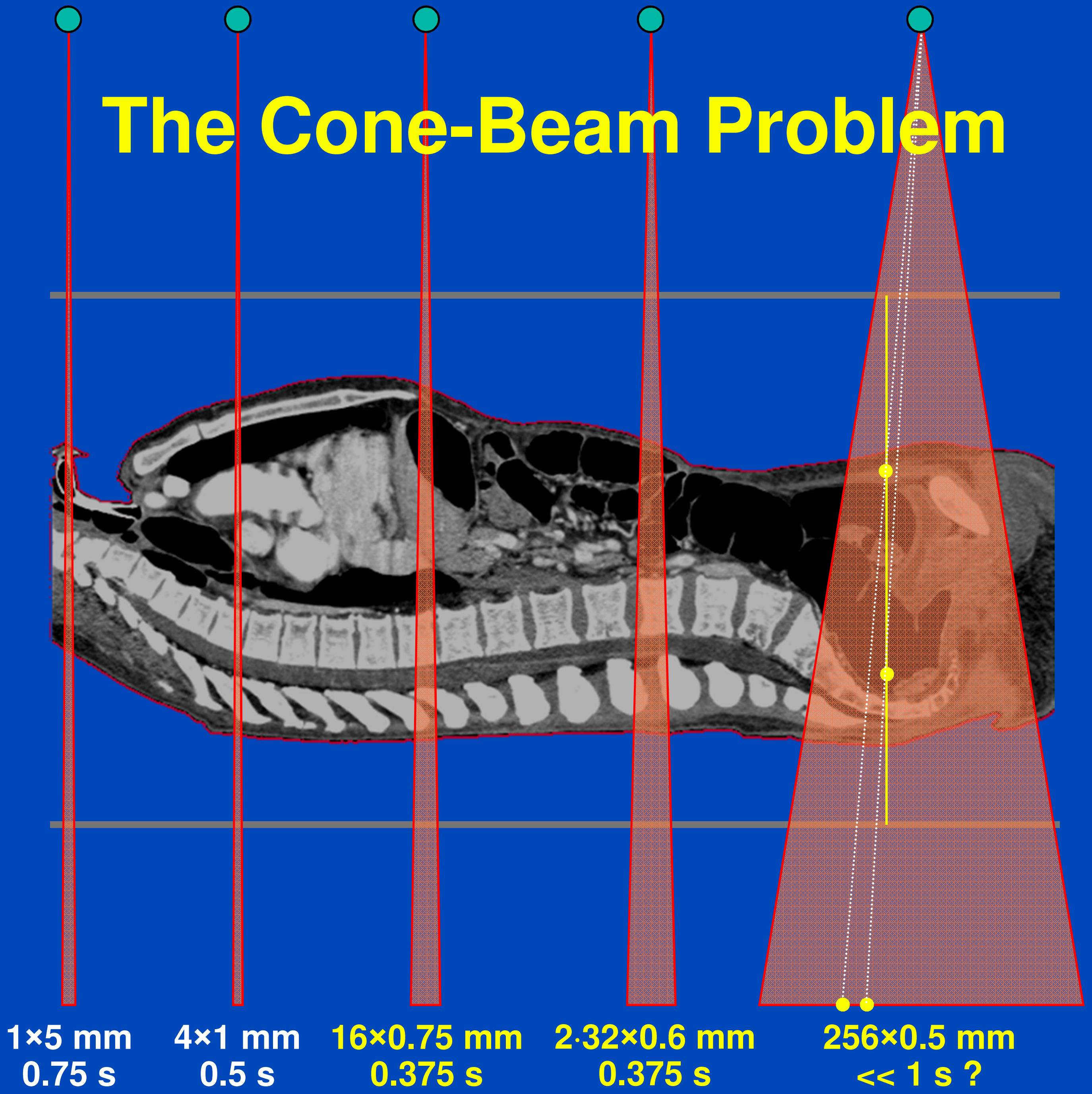

Advanced single-slice rebinning in cone-beam spiral CT

Marc Kachelrieß[a)]
Institute of Medical Physics, University of Erlangen–Nürnberg, Germany

Stefan Schaller
Siemens AG, Medical Engineering Group, Forchheim, Germany

Willi A. Kalender
Institute of Medical Physics, University of Erlangen–Nürnberg, Germany

(Received 11 August 1999; accepted for publication 12 January 2000)

To achieve higher volume coverage at improved *z*-resolution in computed tomography (CT), systems with a large number of detector rows are demanded. However, handling an increased number of detector rows, as compared to today's four-slice scanners, requires to accounting for the cone geometry of the beams. Many so-called cone-beam reconstruction algorithms have been proposed during the last decade. None met all the requirements of the medical spiral cone-beam CT in regard to the need for high image quality, low patient dose and low reconstruction times. We therefore propose an approximate cone-beam algorithm which uses virtual reconstruction planes tilted to optimally fit 180° spiral segments, i.e., the advanced single-slice rebinning (ASSR) algorithm. Our algorithm is a modification of the single-slice rebinning algorithm proposed by Noo *et al.* [Phys. Med. Biol. **44**, 561–570 (1999)] since we use tilted reconstruction slices instead of transaxial slices to approximate the spiral path. Theoretical considerations as well as the reconstruction of simulated phantom data in comparison to the gold standard 180°LI (single-slice spiral CT) were carried out. Image artifacts, *z*-resolution as well as noise levels were evaluated for all simulated scanners. Even for a high number of detector rows the artifact level in the reconstructed images remains comparable to that of 180°LI. Multiplanar reformations of the Defrise phantom show none of the typical cone-beam artifacts usually appearing when going to larger cone angles. Image noise as well as the shape of the respective slice sensitivity profiles are equivalent to the single-slice spiral reconstruction, *z*-resolution is slightly decreased. The ASSR has the potential to become a practical tool for medical spiral cone-beam CT. Its computational complexity lies in the order of standard single-slice CT and it allows to use available 2D backprojection hardware. [S0094-2405(00)00804-X]

Key words: computed tomography (CT), spiral CT, multi-slice CT, cone-beam detector systems, 3D reconstruction

ASSR: Advanced Single-Slice Rebinning

3D and 4D Image Reconstruction for Medium Cone Angles

- First practical solution to the cone-beam problem in medical CT
- Reduction of 3D data to 2D slices
- Commercially implemented as AMPR
- ASSR is recommended for up to 64 slices

Do not confuse
the transmission algorithm ASSR
with
the emission algorithm SSRB!

The ASSR Algorithm

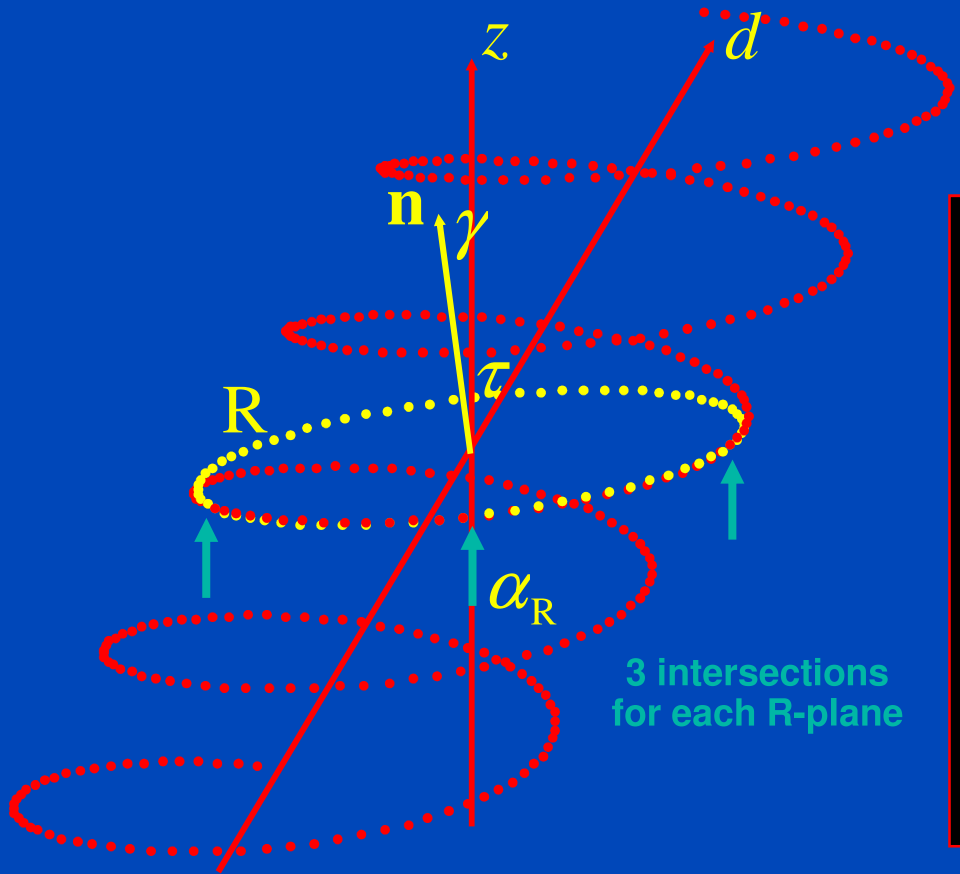

$$p = \frac{d}{MS} \le 1.5$$

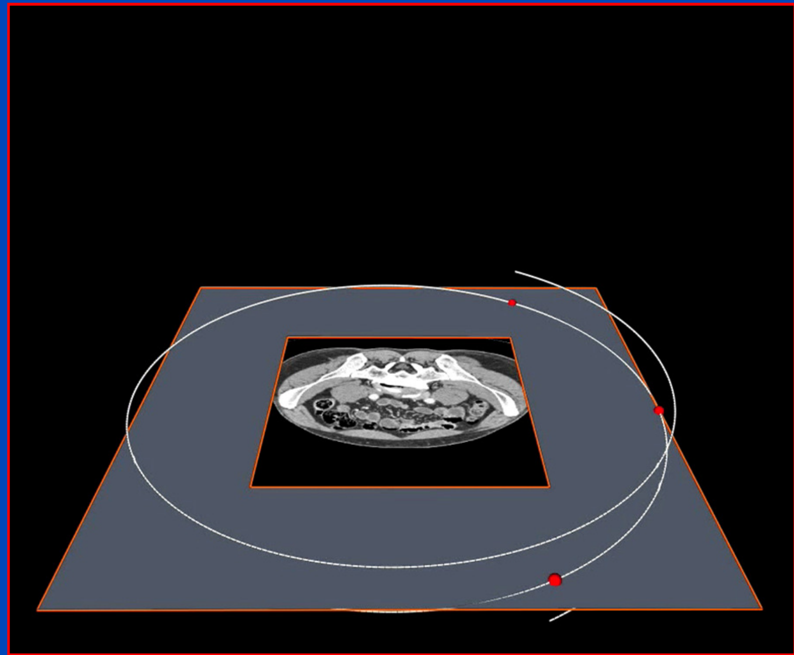

Mean deviation at distance R_M: $\Delta \approx 0.007 \cdot d$

at distance R_F: $\Delta \approx 0.014 \cdot d$

dkfz.

d–Filtering in the Image Domain

- No in-plane interpolations
- Interpolation along *d*
- Arbitrary *d*-filter width

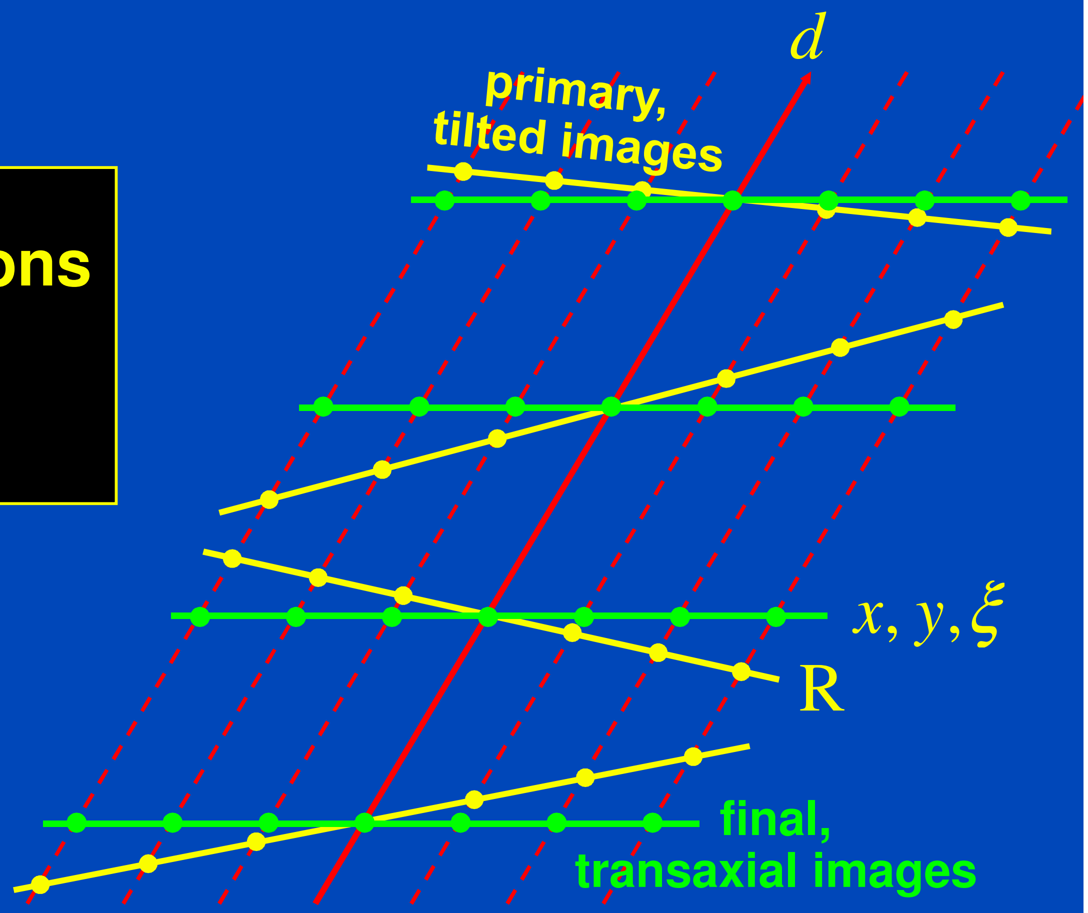

Comparison to Other Approximate Algorithms

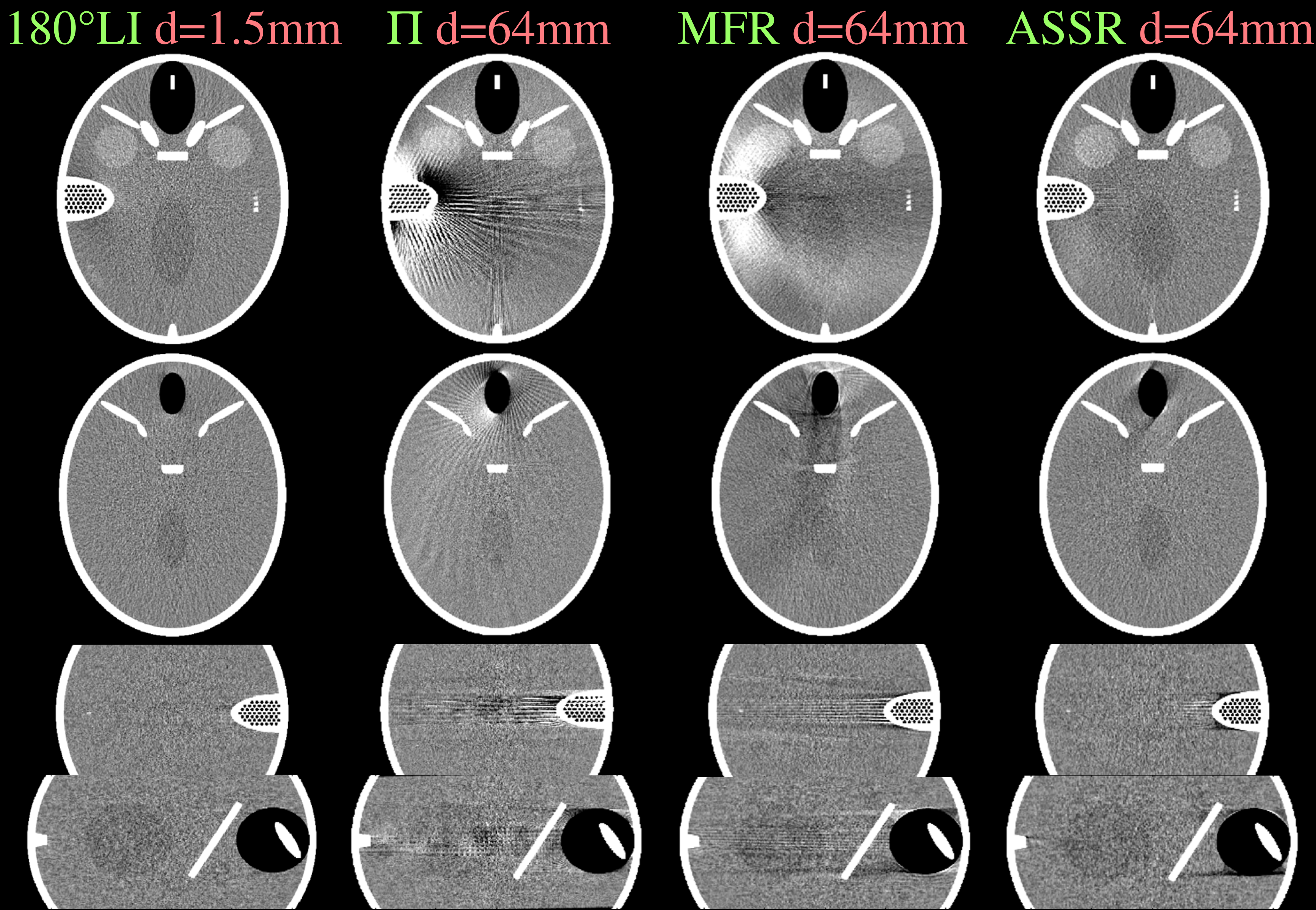

H. Bruder, M. Kachelrieß, S. Schaller. SPIE Med. Imag. Conf. Proc., 3979, 2000

Patient Images with ASSR

- High image quality
- High performance
- Use of available 2D reconstruction hardware
- 100% detector usage
- Arbitrary pitch

- Sensation 16
- 0.5 s rotation
- 16×0.75 mm collimation
- pitch 1.0
- 70 cm in 29 s
- 1.4 GB rawdata
- 1400 images

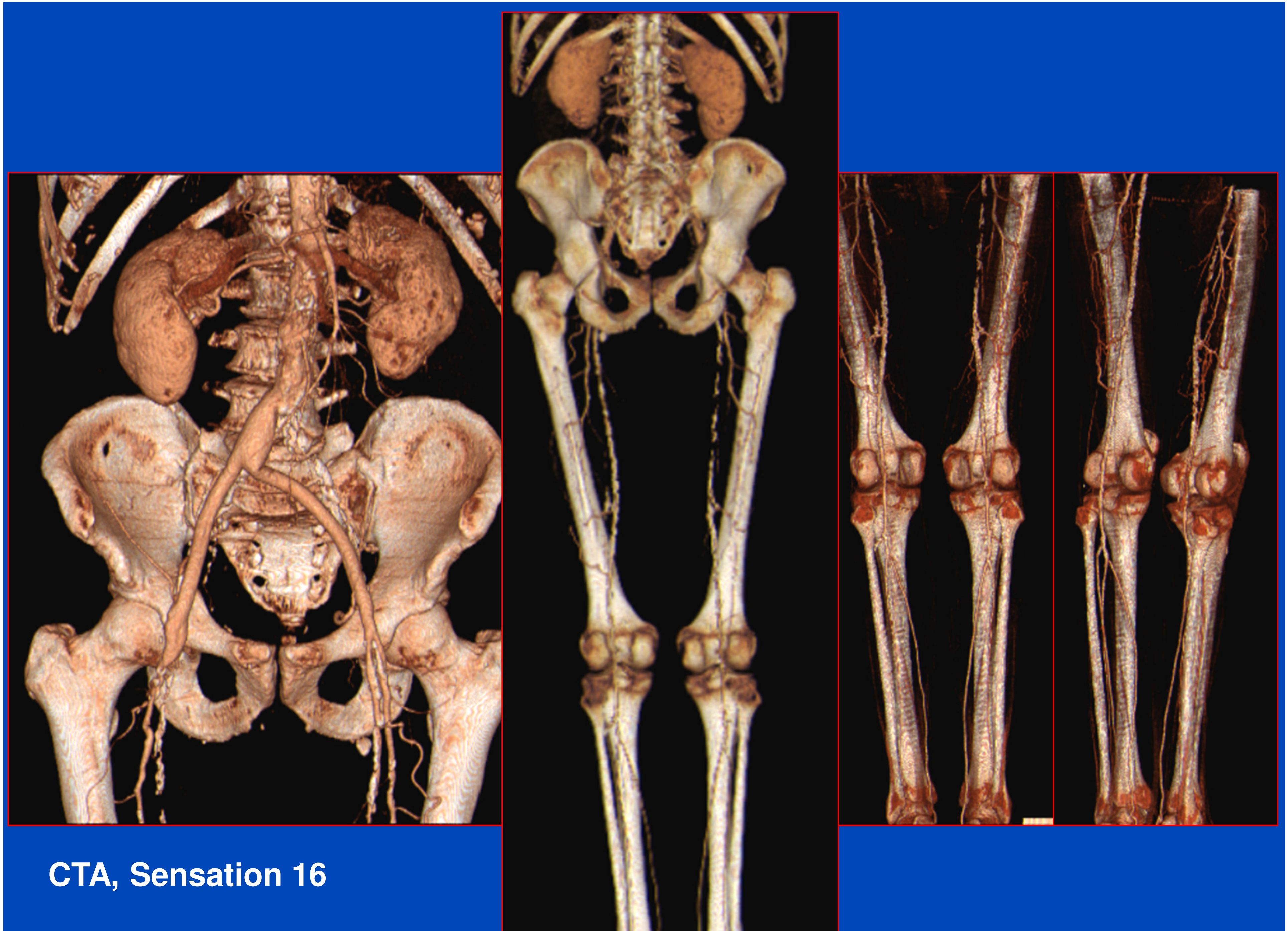

CTA, Sensation 16

Data courtesy of Dr. Michael Lell, Erlangen, Germany

CT-Angiography

Sensation 64 spiral scan with 2·32×0.6 mm and 0.375 s

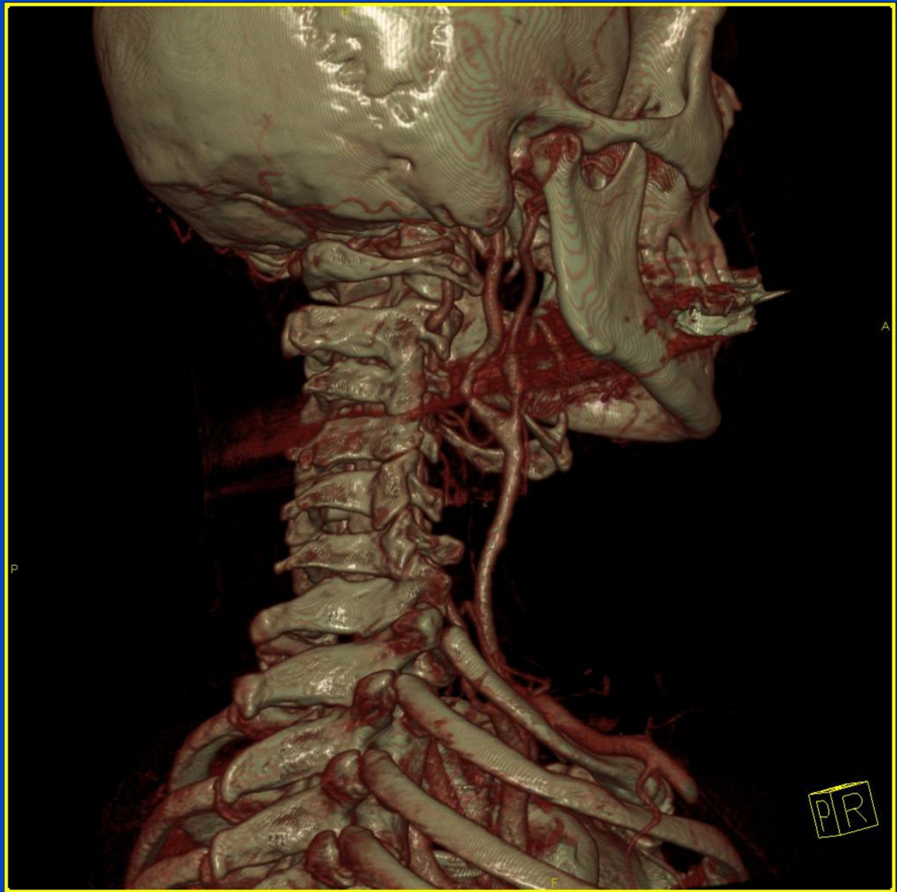

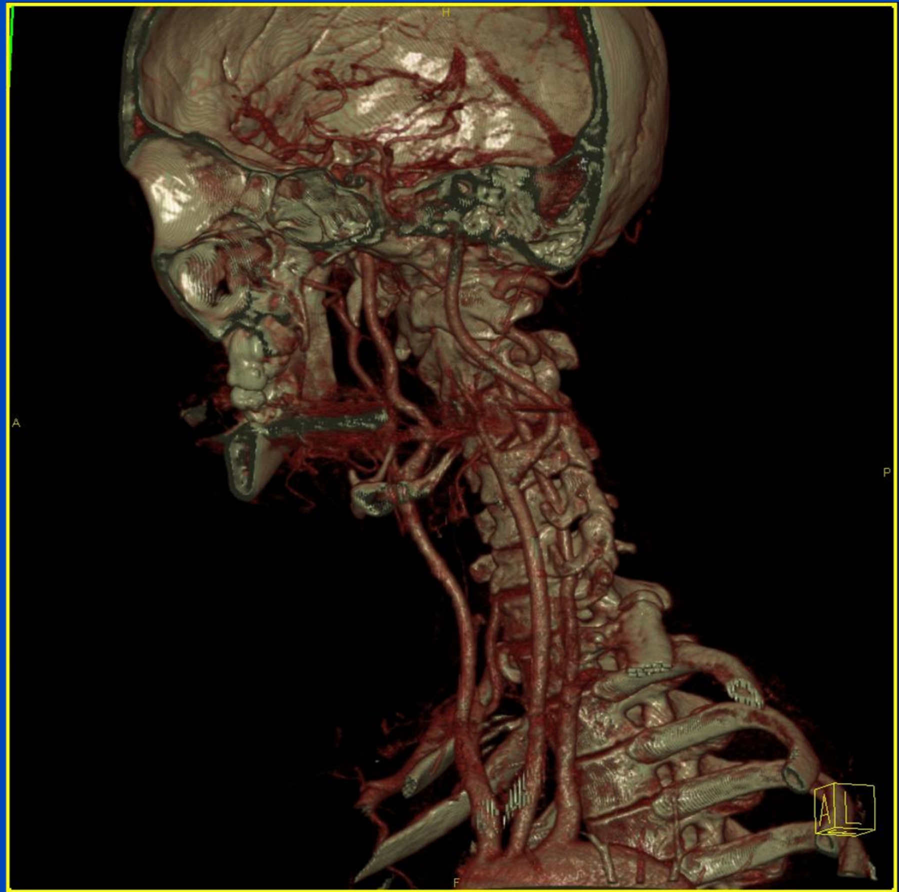

Feldkamp-Type Reconstruction

- **Approximate**
- **Similar to 2D reconstruction:**
  - row-wise filtering of the rawdata
  - followed by backprojection
- **True 3D volumetric backprojection along the original ray direction**
- **Compared to ASSR:**
  - larger cone-angles possible
  - lower reconstruction speed
  - requires 3D backprojection hardware

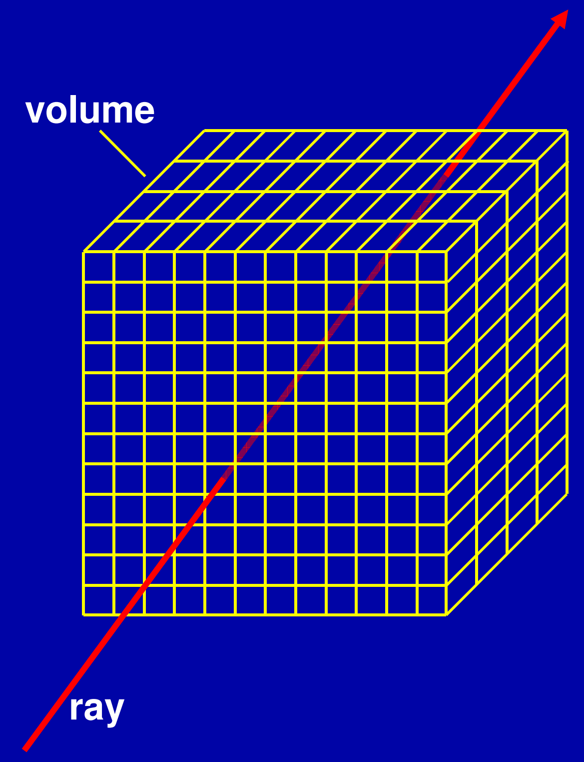

3D backprojection

Extended parallel backprojection for standard three-dimensional and phase-correlated four-dimensional axial and spiral cone-beam CT with arbitrary pitch, arbitrary cone-angle, and 100% dose usage

Marc Kachelrieß,[a)] Michael Knaup, and Willi A. Kalender
Institute of Medical Physics, University of Erlangen—Nürnberg, Germany

(Received 12 September 2003; revised 7 April 2004; accepted for publication 7 April 2004; published 27 May 2004)

We have developed a new approximate Feldkamp-type algorithm that we call the extended parallel backprojection (EPBP). Its main features are a phase-weighted backprojection and a voxel-by-voxel 180° normalization. The first feature ensures three-dimensional (3-D) and 4-D capabilities with one and the same algorithm; the second ensures 100% detector usage (each ray is accounted for). The algorithm was evaluated using simulated data of a thorax phantom and a cardiac motion phantom for scanners with up to 256 slices. Axial (circle and sequence) and spiral scan trajectories were investigated. The standard reconstructions (EPBPStd) are of high quality, even for as many as 256 slices. The cardiac reconstructions (EPBPCI) are of high quality as well and show no significant deterioration of objects even far off the center of rotation. Since EPBPCI uses the cardio interpolation (CI) phase weighting the temporal resolution is equivalent to that of the well-established single-slice and multislice cardiac approaches 180°CI, 180°MCI, and ASSRCI, respectively, and lies in the order of 50 to 100 ms for rotation times between 0.4 and 0.5 s. EPBP appears to fulfill all required demands. Especially the phase-correlated EPBP reconstruction of cardiac multiple circle scan data is of high interest, e.g., for dynamic perfusion studies of the heart. [DOI: 10.1118/1.1755569]

Key words: Cone-beam CT (CBCT), cardiac imaging, 4-D reconstruction, image quality

I. INTRODUCTION

The ongoing development of medical cone-beam CT (CBCT) scanners requires providing cone-beam reconstruction algorithms adequate for medical purposes. These must

adopted and used to reconstruct cardiac data for scanners with more than four slices.

However, there are several restrictions to these approaches that may inhibit their use in scanners with signifi-

Extended Parallel Backprojection (EPBP)

3D and 4D Feldkamp-Type Image Reconstruction for Large Cone Angles

- Trajectories: circle, sequence, spiral
- Scan modes: standard, phase-correlated
- Rebinning: azimuthal + longitudinal + radial
- Feldkamp-type: convolution + true 3D backprojection
- 100% detector usage
- Fast and efficient

Kachelrieß et al., Med. Phys. 31(6), June 2006

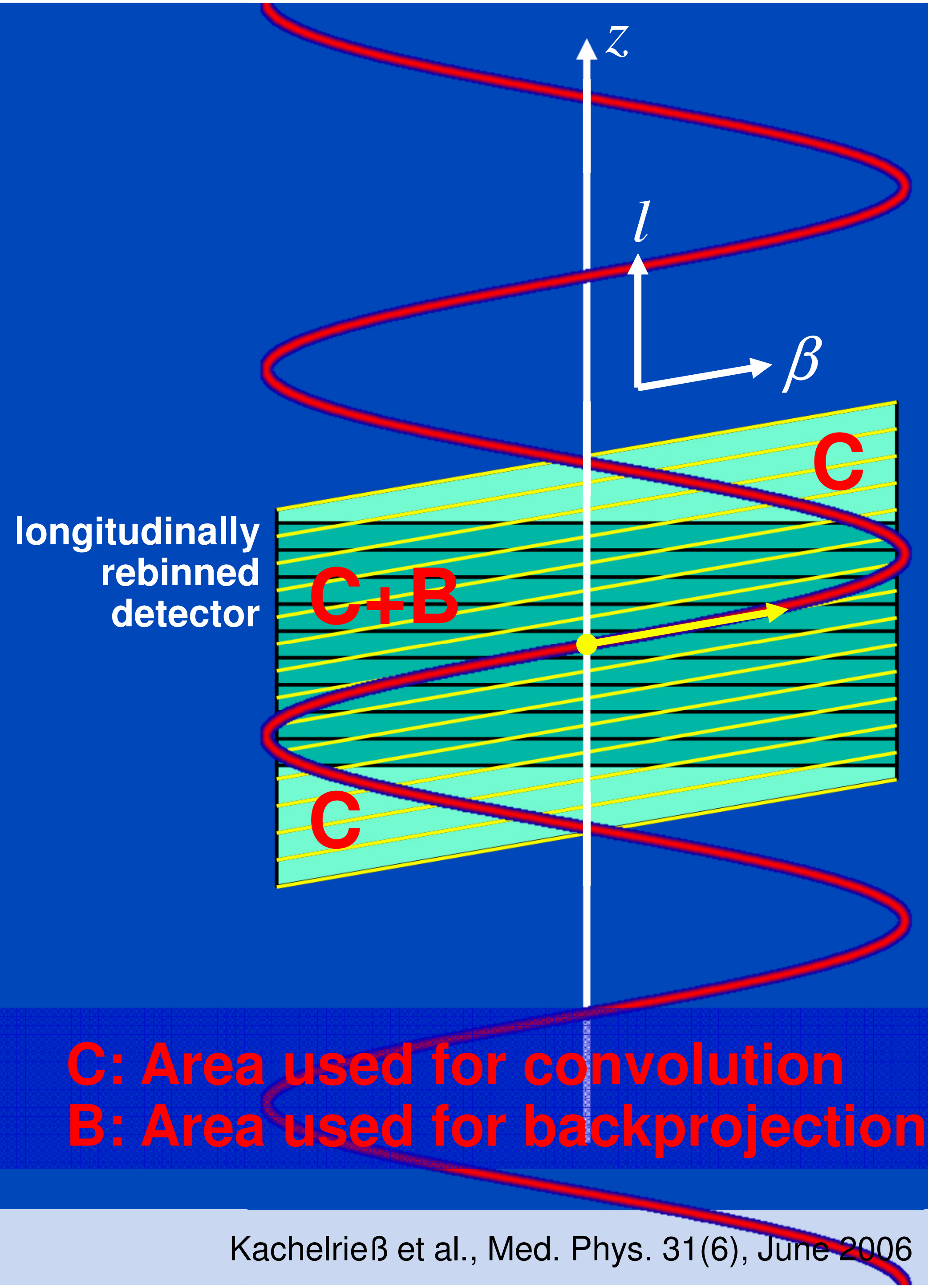

$$p = \frac{d}{MS} \leq 1.5$$

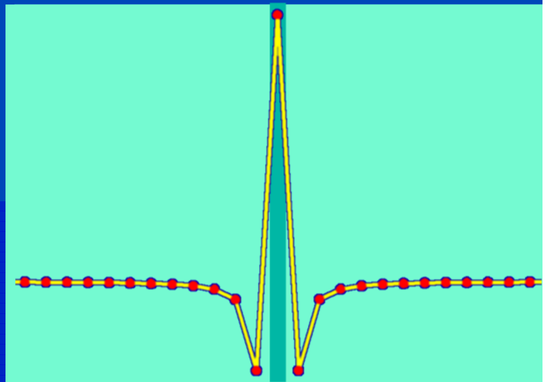

C: Area used for convolution
B: Area used for backprojection

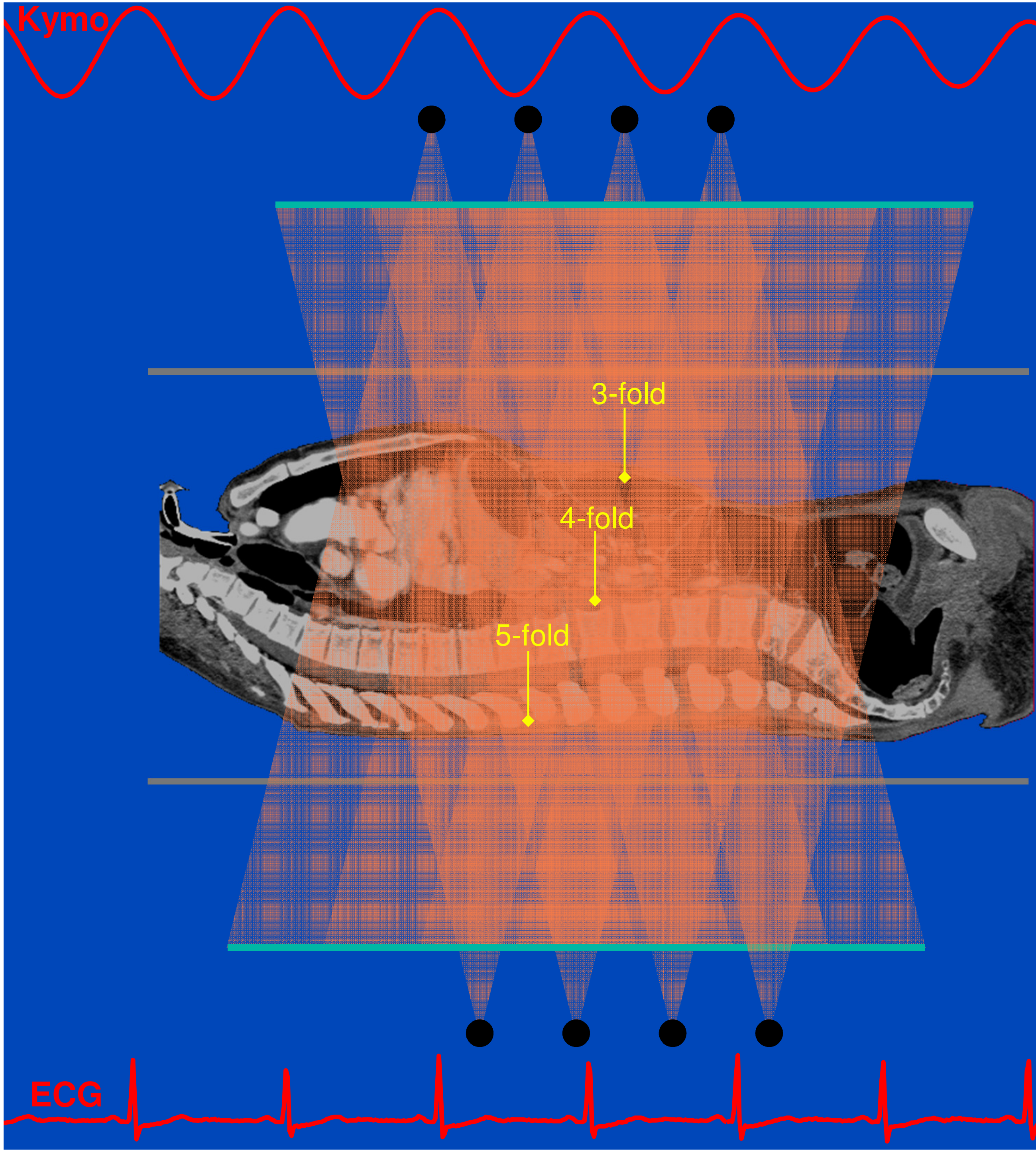

The complicated pattern of overlapping data …

… will become even more complicated with phase-correlation.

⇒ Individual voxel-by-voxel weighting and normalization.

The 180° Condition

$$\int d\vartheta\, w(\vartheta) = \pi$$

and

$$\sum_k w(\vartheta + k\pi) = 1$$

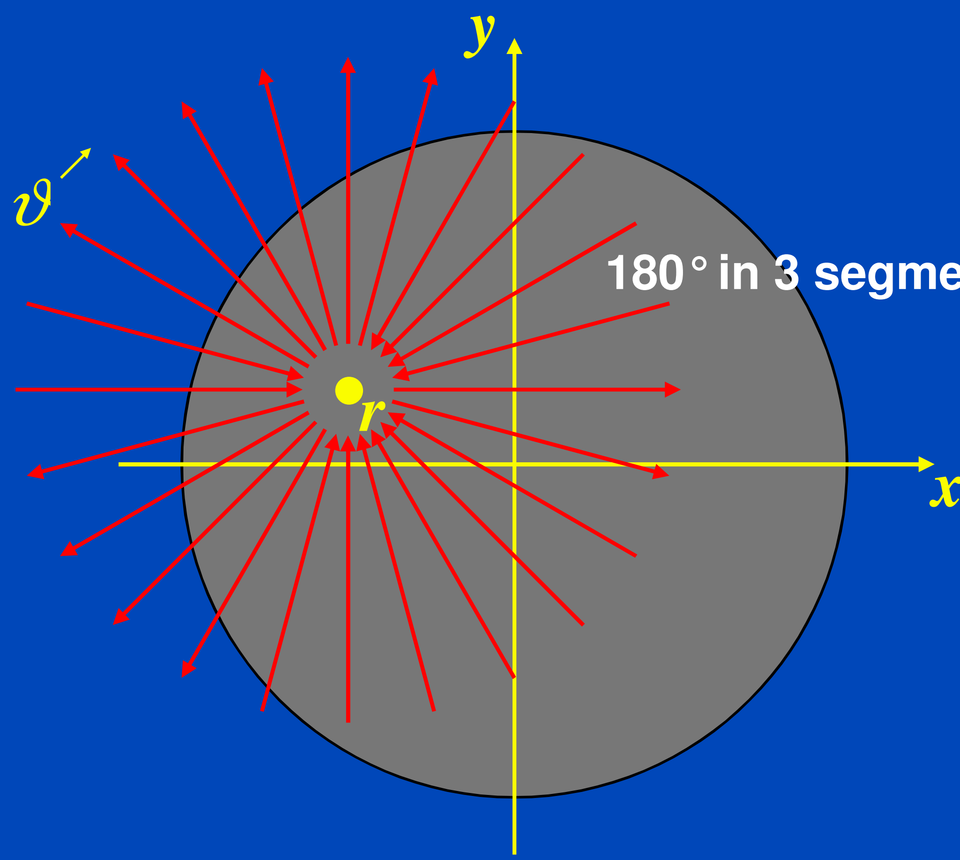

The (weighted) contributions to each object point must make up an interval of 180° and weight 1.

- **Spiral**
- **EPBP Std**
- ***p* = 0.375**

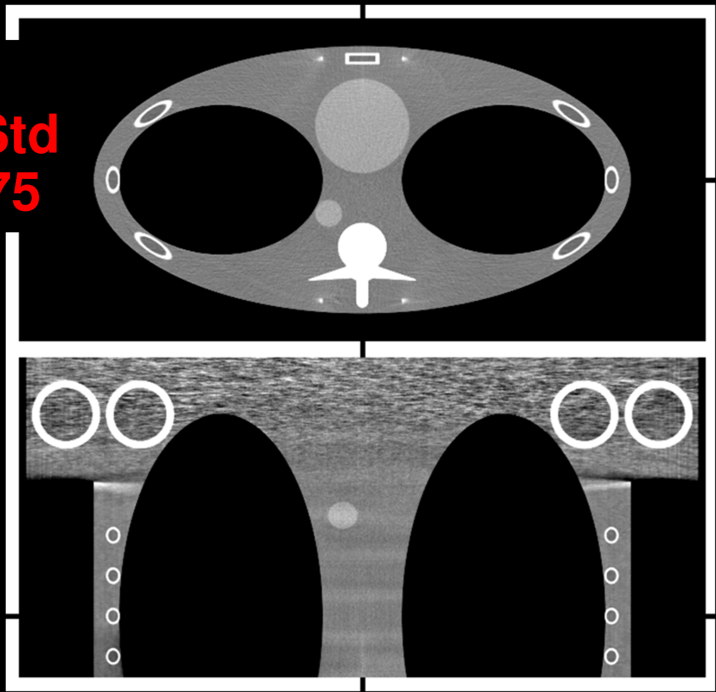

- **Spiral**
- **EPBP Std**
- ***p* = 1.0**

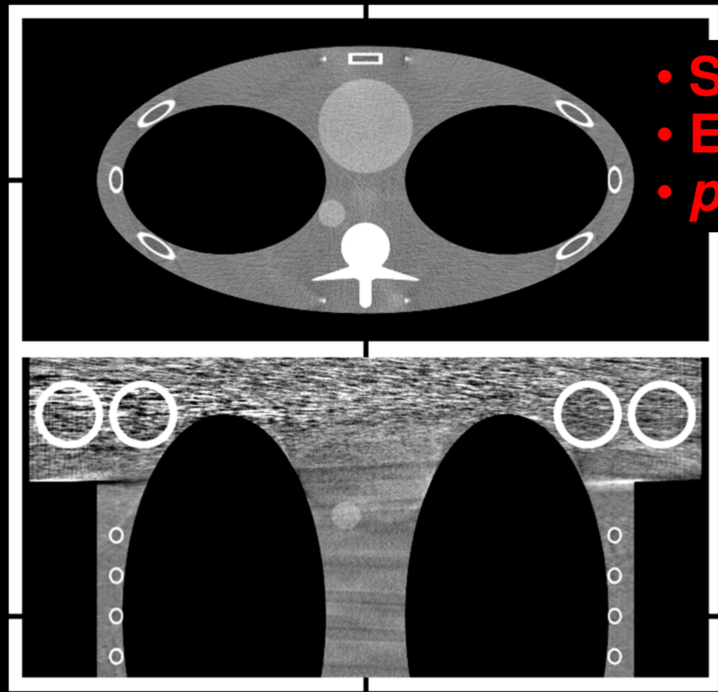

- **Spiral**
- **ASSR Std**
- ***p* = 1.0**

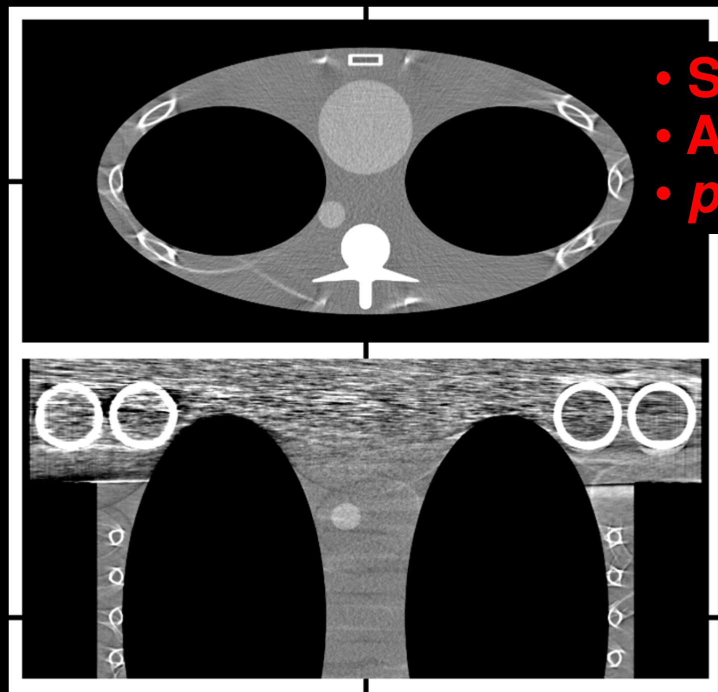

- **256 slices**
- **(0/300)**

Kachelrieß et al., Med. Phys. 31(6): 1623-1641, 2004

Patient example, 32x0.6 mm, z-FFS, p=0.23, t_{rot}=0.375 s.

Iterative Image Reconstruction

$$x^2 = y$$

Model

$$\cancel{x = \sqrt{y}}$$

$$(x_n + \Delta x_n)^2 = y$$

$$x_n^2 + 2x_n\Delta x_n + \cancel{\Delta x_n^2} = y$$

$$x_n^2 + 2x_n\Delta x_n \approx y$$

$$\Delta x_n = \tfrac{1}{2}(y - x_n^2)/x_n$$

$$x_{n+1} = x_n + \Delta x_n$$

Update equation

This is an iterative solution.

dkfz.

Influence of Update Equation and Model

$0.5\,(3 - x_n^2)/x_n$	$0.4\,(3 - x_n^2)/x_n$	$0.5\,(3 - x_n^{2.1})/x_n$
$x_0 = 1.$	$x_0 = 1.$	$x_0 = 1.$
$x_1 = 2.$	$x_1 = 1.8$	$x_1 = 2.$
$x_2 = 1.75$	$x_2 = 1.74667$	$x_2 = 1.67823$
$x_3 = 1.73214$	$x_3 = 1.73502$	$x_3 = 1.68833$
$x_4 = 1.73205$	$x_4 = 1.73265$	$x_4 = 1.68723$
$x_5 = 1.73205$	$x_5 = 1.73217$	$x_5 = 1.68734$
$x_6 = 1.73205$	$x_6 = 1.73207$	$x_6 = 1.68733$
$x_7 = 1.73205$	$x_7 = 1.73206$	$x_7 = 1.68733$
$x_8 = 1.73205$	$x_8 = 1.73205$	$x_8 = 1.68733$

$$x^2 = 3, \quad x_0 = 1, \quad x_{n+1} = x_n + \Delta x_n$$

Analytische Rekonstruktion

1. Problem $$p(\vartheta,\xi) = \int dxdy\, f(x,y)\delta(x\cos\vartheta + y\sin\vartheta - \xi)$$

2. Lösungsformel $$f(x,y) = \int_0^\pi d\vartheta\, p(\vartheta,\xi) * k(\xi)\Big|_{\xi = x\cos\vartheta + y\sin\vartheta}$$

3. Diskretisierung $$\boldsymbol{f} = \boldsymbol{R}^{\mathrm{T}} \cdot \boldsymbol{K} \cdot \boldsymbol{p} = \boldsymbol{R}^{\mathrm{T}} \cdot (\boldsymbol{k} * \boldsymbol{p})$$

Klassische iterative Rekonstruktion

1. Problem $$p(\vartheta,\xi) = \int dxdy\, f(x,y)\delta(x\cos\vartheta + y\sin\vartheta - \xi)$$

2. Diskretisierung $$\boldsymbol{p} = \boldsymbol{R} \cdot \boldsymbol{f}$$

3. Lösungsformel $$\boldsymbol{f}_{\nu+1} = \boldsymbol{f}_{\nu} + \boldsymbol{R}^{\mathrm{T}} \cdot \frac{\boldsymbol{p} - \boldsymbol{R} \cdot \boldsymbol{f}_{\nu}}{\boldsymbol{R}^2 \cdot \boldsymbol{1}}$$

dkfz.

CT System Matrix

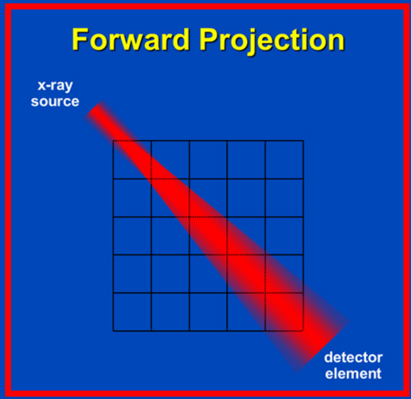

$$\underbrace{\boldsymbol{R}}_{\text{Radon or x-ray transform}} \cdot \underbrace{\boldsymbol{f}}_{\text{image to be reconstructed}} = \underbrace{\boldsymbol{p}}_{\text{measured rawdata}}$$

$$\boldsymbol{R} = \begin{pmatrix} r_{11} & r_{12} & \cdots & r_{1M} \\ r_{21} & r_{22} & \cdots & r_{2M} \\ \vdots & \vdots & \ddots & \vdots \\ r_{N1} & r_{N2} & \cdots & r_{NM} \end{pmatrix}, \quad \boldsymbol{f} = \begin{pmatrix} f_1 \\ f_2 \\ \vdots \\ f_M \end{pmatrix}, \quad \boldsymbol{p} = \begin{pmatrix} p_1 \\ p_2 \\ \vdots \\ p_N \end{pmatrix}$$

Kaczmarz‘s Method

$$\underbrace{\boldsymbol{R}}_{N \times M} \cdot \underbrace{\boldsymbol{f}}_{M \times 1} = \underbrace{\boldsymbol{p}}_{N \times 1}$$

$$\boldsymbol{R} = \begin{pmatrix} \boldsymbol{r}_1 \\ \boldsymbol{r}_2 \\ \vdots \\ \boldsymbol{r}_N \end{pmatrix}, \quad |\boldsymbol{r}_n| = 1$$

$$\boldsymbol{r}_n \cdot \boldsymbol{f} = p_n$$

Kaczmarz‘s Method (2)

- Successively solve $\boldsymbol{r}_n \cdot \boldsymbol{f} = p_n$
- To do so, project onto the hyperplanes

$$\boldsymbol{r}_n \cdot \big(\boldsymbol{f} + \lambda \boldsymbol{r}_n\big) = p_n$$

$$\lambda = p_n - \boldsymbol{r}_n \cdot \boldsymbol{f}$$

$$\boldsymbol{f}_{\text{new}} = \boldsymbol{f} + \lambda \boldsymbol{r}_n$$

$$\boldsymbol{f}_{\text{new}} = \boldsymbol{f} + \boldsymbol{r}_n \big(p_n - \boldsymbol{r}_n \cdot \boldsymbol{f}\big)$$

- Repeat until some convergence criterion is reached

$$\boldsymbol{f}_{\nu+1} = \boldsymbol{f}_\nu + \boldsymbol{r}_n \big(p_n - \boldsymbol{r}_n \cdot \boldsymbol{f}_\nu\big)$$

Kaczmarz‘s Method (3)

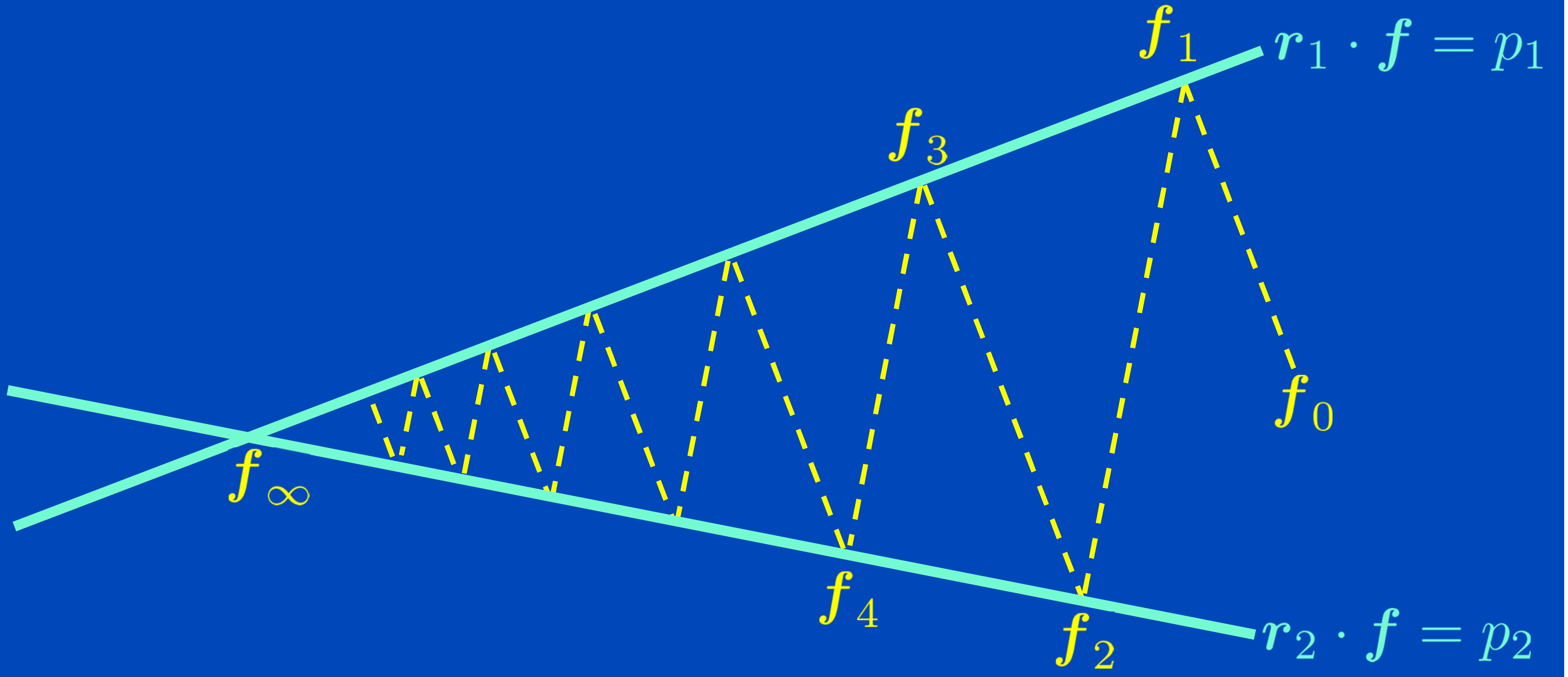

$$\boldsymbol{f}_{\nu+1} = \boldsymbol{f}_\nu + \boldsymbol{r}_n \big(p_n - \boldsymbol{r}_n \cdot \boldsymbol{f}_\nu\big)$$

Kaczmarz in Image Reconstruction: Algebraic Reconstruction Technique (ART)

$$\boldsymbol{f}_{\nu+1} = \boldsymbol{f}_\nu + \boldsymbol{r}_n \big(p_n - \boldsymbol{r}_n \cdot \boldsymbol{f}_\nu \big)$$

$$\boxed{\boldsymbol{f}_{\nu+1} = \boldsymbol{f}_\nu + \boldsymbol{R}^{\mathrm{T}} \cdot \frac{\boldsymbol{p} - \boldsymbol{R} \cdot \boldsymbol{f}_\nu}{\boldsymbol{R}^2 \cdot \boldsymbol{1}}}$$

dkfz.

Kaczmarz‘s Method = ART

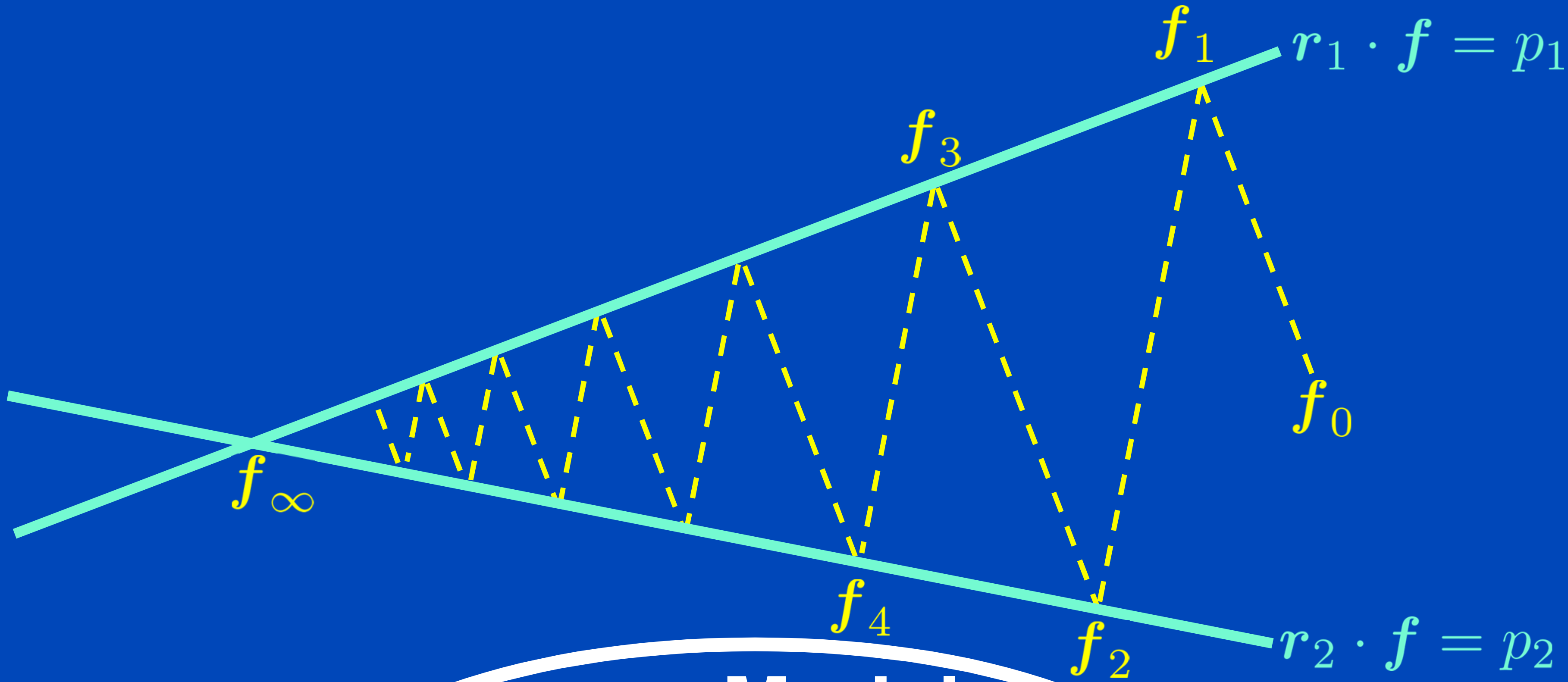

Model

$$\boldsymbol{f}_{\nu+1} = \boldsymbol{f}_\nu + \boldsymbol{R}^{\mathrm{T}} \cdot \frac{\boldsymbol{p} - \boldsymbol{R} \cdot \boldsymbol{f}_\nu}{\boldsymbol{R}^2 \cdot \boldsymbol{1}}$$

Update equation

Kaczmarz‘s Method = ART

$$\boldsymbol{f}_{\nu+1} = \boldsymbol{f}_{\nu} + \boldsymbol{R}^{\mathrm{T}} \cdot \frac{\boldsymbol{p} - \boldsymbol{R} \cdot \boldsymbol{f}_{\nu}}{\boldsymbol{R}^{2} \cdot \boldsymbol{1}}$$

apply inverse model

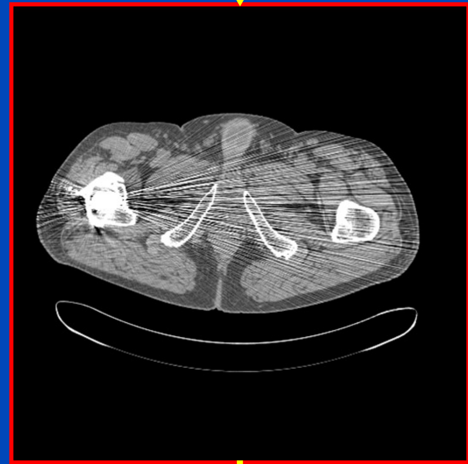

apply forward model

$$\boldsymbol{f}_{\nu+1} = \boldsymbol{f}_{\nu} + \boldsymbol{R}^{\mathrm{T}} \cdot \frac{\boldsymbol{p} - \boldsymbol{R} \cdot \boldsymbol{f}_{\nu}}{\boldsymbol{R}^2 \cdot \mathbf{1}}$$

Direct vs. Filtered Backprojection

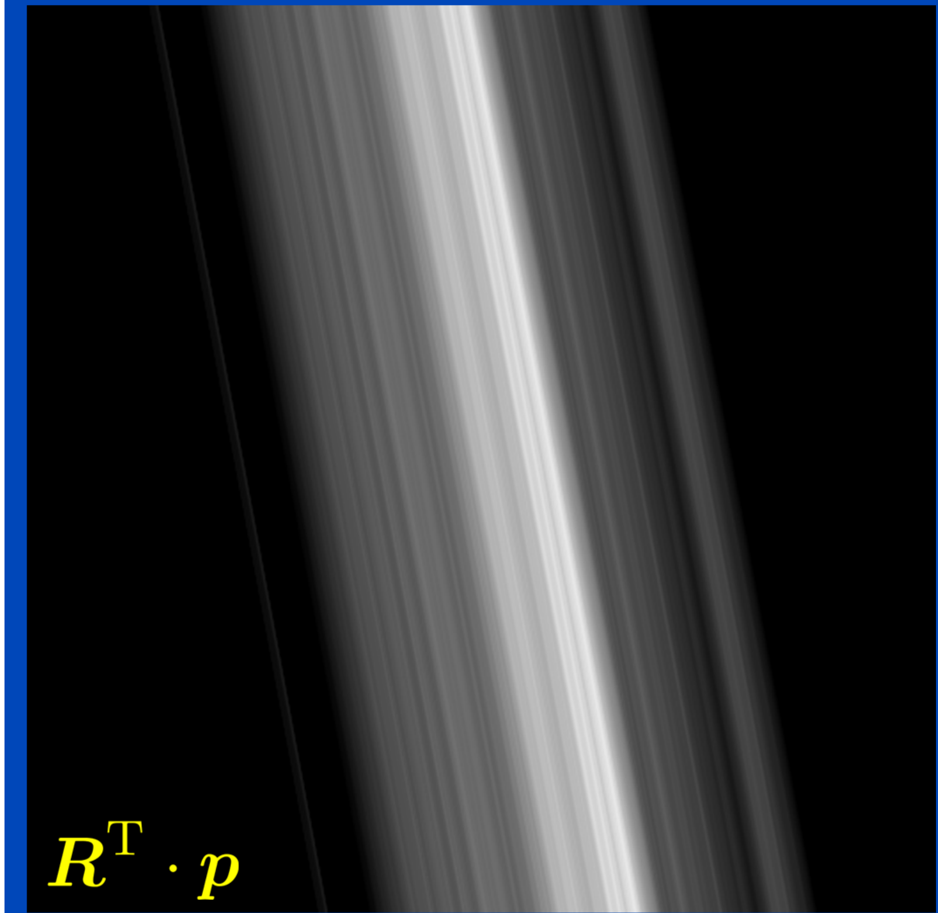

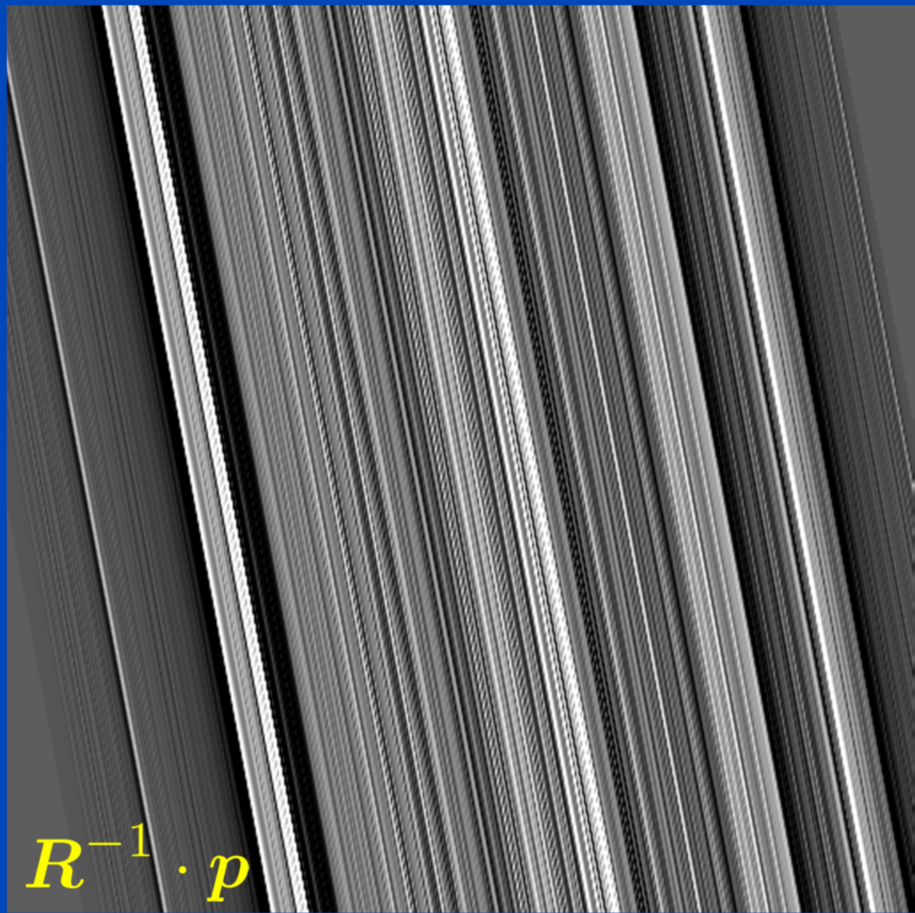

Flavours of Iterative Reconstruction

- **ART** $$\boldsymbol{f}_{\nu+1} = \boldsymbol{f}_\nu + \boldsymbol{R}^{\mathrm{T}} \cdot \frac{\boldsymbol{p} - \boldsymbol{R} \cdot \boldsymbol{f}_\nu}{\boldsymbol{R}^2 \cdot \boldsymbol{1}}$$
- **SART** $$\boldsymbol{f}_{\nu+1} = \boldsymbol{f}_\nu + \frac{1}{\boldsymbol{R}^{\mathrm{T}} \cdot \boldsymbol{1}} \boldsymbol{R}^{\mathrm{T}} \cdot \frac{\boldsymbol{p} - \boldsymbol{R} \cdot \boldsymbol{f}_\nu}{\boldsymbol{R} \cdot \boldsymbol{1}}$$
- **MLEM** $$\boldsymbol{f}_{\nu+1} = \boldsymbol{f}_\nu \frac{\boldsymbol{R}^{\mathrm{T}} \cdot \left(e^{-\boldsymbol{R} \cdot \boldsymbol{f}_\nu}\right)}{\boldsymbol{R}^{\mathrm{T}} \cdot \left(e^{-\boldsymbol{p}}\right)}$$
- **OSC** $$\boldsymbol{f}_{\nu+1} = \boldsymbol{f}_\nu + \boldsymbol{f}_\nu \frac{\boldsymbol{R}^{\mathrm{T}} \cdot \left(e^{-\boldsymbol{R} \cdot \boldsymbol{f}_\nu} - e^{-\boldsymbol{p}}\right)}{\boldsymbol{R}^{\mathrm{T}} \cdot \left(e^{-\boldsymbol{R} \cdot \boldsymbol{f}_\nu} \boldsymbol{R} \cdot \boldsymbol{f}_\nu\right)}$$
- **and hundreds more …**

Cost Functions

- **General expression:** $\boldsymbol{f} = \arg\min_{\boldsymbol{f}} C(\boldsymbol{f})$

- **Examples:**

$$C(\boldsymbol{f}) = \left(\boldsymbol{R}\cdot\boldsymbol{f} - \boldsymbol{p}\right)^2$$

$$C(\boldsymbol{f}) = \left(\boldsymbol{W}\cdot(\boldsymbol{R}\cdot\boldsymbol{f} - \boldsymbol{p})\right)^2$$

$$C(\boldsymbol{f}) = \left(\underset{\substack{\uparrow\\ \text{statistical properties and preconditioning}}}{\boldsymbol{W}}\cdot(\boldsymbol{R}\cdot\boldsymbol{f} - \boldsymbol{p})\right)^2 + \beta \underset{\substack{\uparrow\\ \text{additional penalties}}}{P(\boldsymbol{f})}$$

statistical properties and **preconditioning**

additional penalties

Linear PWLS

PWLS $$C(\boldsymbol{f}) = (\boldsymbol{R}\cdot\boldsymbol{f}-\boldsymbol{p})^{\mathrm{T}}\cdot\boldsymbol{W}\cdot(\boldsymbol{R}\cdot\boldsymbol{f}-\boldsymbol{p})+\beta\boldsymbol{f}^{\mathrm{T}}\cdot\boldsymbol{Q}\cdot\boldsymbol{f}$$

Gradient $$\boldsymbol{\nabla}C(\boldsymbol{f}) \propto \boldsymbol{R}^{\mathrm{T}}\cdot\boldsymbol{W}\cdot(\boldsymbol{R}\cdot\boldsymbol{f}-\boldsymbol{p})+\beta\boldsymbol{Q}\cdot\boldsymbol{f}$$

Gradient update $$f_{\nu+1} = f_\nu - \alpha_\nu\boldsymbol{\nabla}C(\boldsymbol{f}_\nu)$$

At convergence $$\boldsymbol{\nabla}C(\boldsymbol{f}_\infty) = 0$$

Fixed point $$\boldsymbol{f}_\infty = (\boldsymbol{R}^{\mathrm{T}}\cdot\boldsymbol{W}\cdot\boldsymbol{R}+\beta\boldsymbol{Q})^{-1}\cdot\boldsymbol{R}^{\mathrm{T}}\cdot\boldsymbol{W}\cdot\boldsymbol{p}$$

Assume there exists $\hat{f}$ such that $R\cdot\hat{f}=p$. Then everything reduces to a shift variant image filter:

$$\boldsymbol{f}_\infty = (\boldsymbol{R}^{\mathrm{T}}\cdot\boldsymbol{W}\cdot\boldsymbol{R}+\beta\boldsymbol{Q})^{-1}\cdot\boldsymbol{R}^{\mathrm{T}}\cdot\boldsymbol{W}\cdot\boldsymbol{R}\cdot\hat{\boldsymbol{f}}$$

In case of shift invariance we can convert to Fourier domain:

high-pass

$$\mathsf{F}\boldsymbol{f}_\infty = \frac{1}{1+\beta\frac{\mathsf{F}\boldsymbol{Q}}{\mathsf{F}\boldsymbol{R}^{\mathrm{T}}\cdot\boldsymbol{W}\cdot\boldsymbol{R}}}\mathsf{F}\hat{\boldsymbol{f}}$$

low-pass

Non-Linear PWLS

PWLS $$C(\boldsymbol{f}) = (\boldsymbol{R}\cdot\boldsymbol{f}-\boldsymbol{p})^{\mathrm{T}}\cdot\boldsymbol{W}\cdot(\boldsymbol{R}\cdot\boldsymbol{f}-\boldsymbol{p})+\beta P(\boldsymbol{f})$$

Gradient $$\nabla C(\boldsymbol{f}) \propto \boldsymbol{R}^{\mathrm{T}}\cdot\boldsymbol{W}\cdot(\boldsymbol{R}\cdot\boldsymbol{f}-\boldsymbol{p})+\beta\nabla P(\boldsymbol{f})$$

$$\approx \boldsymbol{Q}(\boldsymbol{f})\cdot\boldsymbol{f}$$

Gradient update $$\boldsymbol{f}_{\nu+1} = \boldsymbol{f}_\nu - \alpha_\nu\nabla C(\boldsymbol{f}_\nu)$$

At convergence $$\nabla C(\boldsymbol{f}_\infty) = 0$$

Fixed point $$\boldsymbol{f}_\infty = (\boldsymbol{R}^{\mathrm{T}}\cdot\boldsymbol{W}\cdot\boldsymbol{R}+\beta\boldsymbol{Q}(\boldsymbol{f}_\infty))^{-1}\cdot\boldsymbol{R}^{\mathrm{T}}\cdot\boldsymbol{W}\cdot\boldsymbol{p}$$

Assume there exists $\hat{f}$ such that $R\cdot\hat{f}=p$. Then everything reduces to a shift variant image filter:

$$\boldsymbol{f}_\infty = (\boldsymbol{R}^{\mathrm{T}}\cdot\boldsymbol{W}\cdot\boldsymbol{R}+\beta\boldsymbol{Q}(\boldsymbol{f}_\infty))^{-1}\cdot\boldsymbol{R}^{\mathrm{T}}\cdot\boldsymbol{W}\cdot\boldsymbol{R}\cdot\hat{\boldsymbol{f}}$$

What Makes Iterative Recon Attractive?

- No need to come find an analytical solution
- Works for all geometries with only small adaptations
- Allows to model any effect
- Allows to incorporate prior knowledge
  - noise properties (quantum noise, electronic noise, noise texture, …)
  - prior scans (e.g. planning CT, full scan data, …)
  - image properties such as smoothness, edges (e.g. minimum TV)
  - …
- Handles missing data implicitly (but not necessarily better)

Phase-correlated Feldkamp

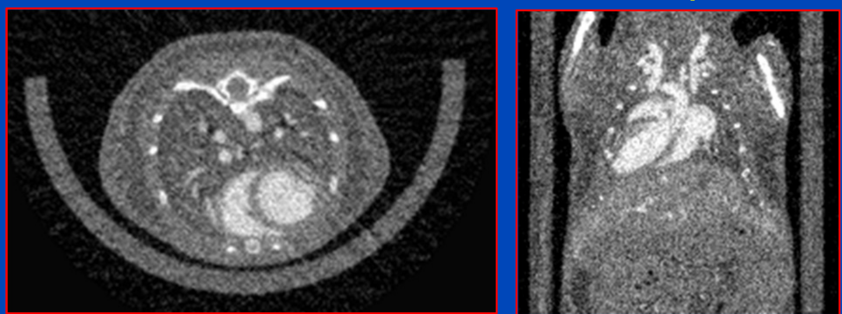

High dimensional TV minimization[1]

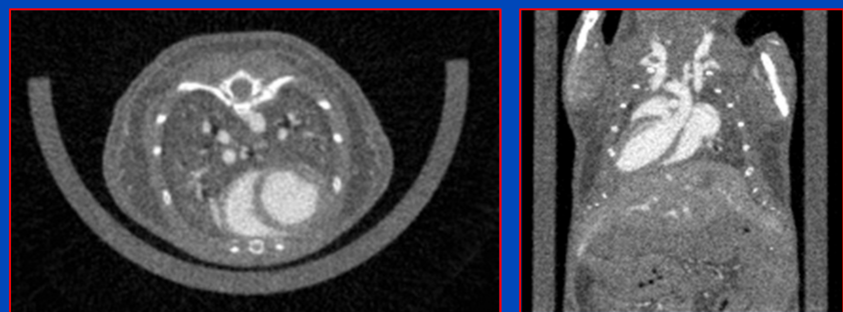

[1] L. Ritschl, S. Sawall, M. Knaup, A. Hess, and M. Kachelrieß, Phys. Med. Biol. 57, Jan. 2012

Downsides

- Classical iterative recon is slow!
- Classical iterative recon cannot do small FOVs.
- There are many open parameters.
- The reconstruction is non-linear.
- Can we trust the images?

Ordered Subsets

- Divide one iteration into *S* sub-iterations.
- Each of these *S* subsets covers *N*/*S* projections.
- During one iteration all subsets and therefore all projections are used exactly once.
- Per iteration the volume is updated *S* times (once per sub-iteration).
- An up to *S*-fold speed-up can be observed.

Ordered Subsets
Illustration for $N = 32$ Projections

Conventional procedure without subets ($S = 1$)

0 1 2 3 4 5 6 7 8 9 10 11 12 13 14 15 16 17 18 19 20 21 22 23 24 25 26 27 28 29 30 31

Ordered subsets with $S = 8$ sub-iterations

0 1 2 3 4 5 6 7 8 9 10 11 12 13 14 15 16 17 18 19 20 21 22 23 24 25 26 27 28 29 30 31

Ordered Subsets

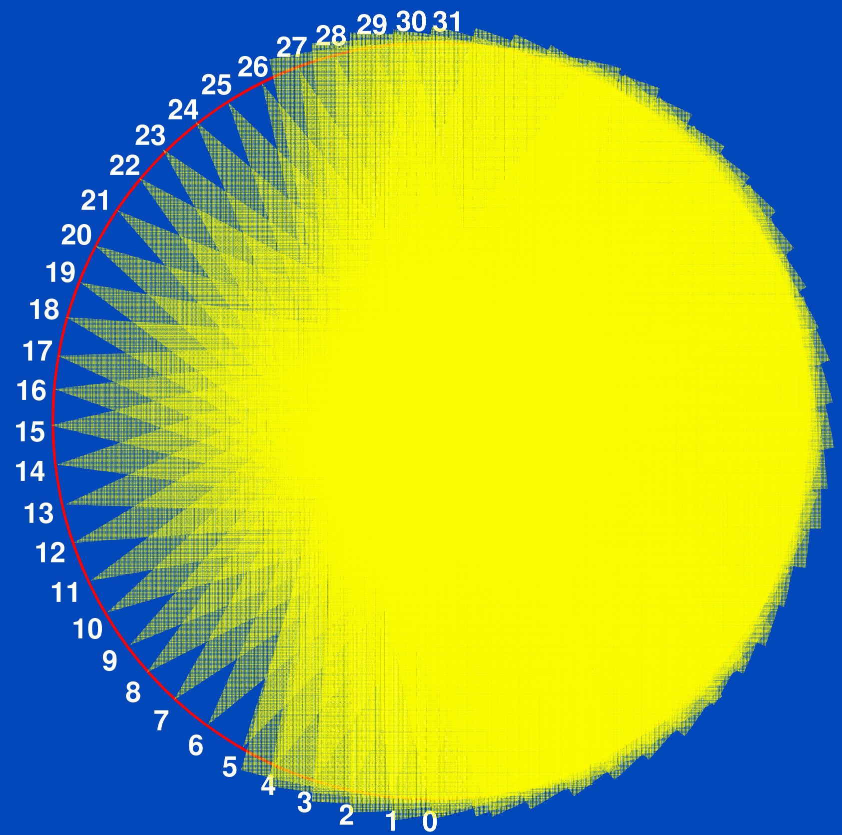

$N_{\text{Projections}}$ = 32, Ordered Subsets: N_{Subsets} = 8

Sequence Can be Generated Using Simple Bit Reversal

0	->	0
1	->	16
2	->	8
3	->	24
4	->	4
5	->	20
6	->	12
7	->	28
8	->	2
9	->	18
10	->	10
11	->	26
12	->	6
13	->	22
14	->	14
15	->	30
16	->	1
17	->	17
18	->	9
19	->	25
20	->	5
21	->	21
22	->	13
23	->	29
24	->	3
25	->	19
26	->	11
27	->	27
28	->	7
29	->	23
30	->	15
31	->	31

Using Ordered Subsets Makes it Faster!

S = 1 (no subsets) | *S* = 32 (ordered subsets)

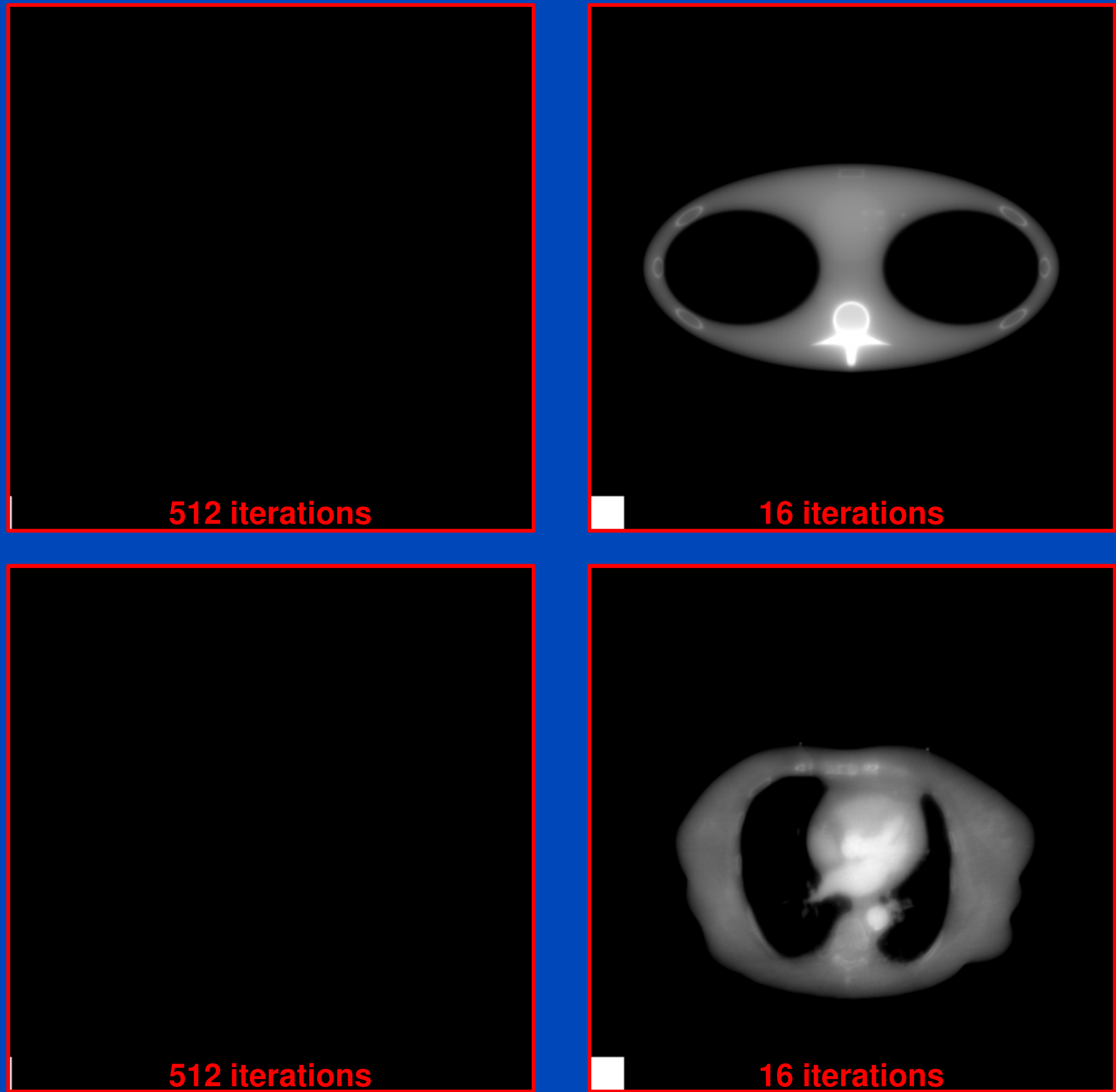

$C = 0$ HU, $W = 1000$ HU

Image Updates

S = 1 (no subsets) | **S = 32 (ordered subsets)**

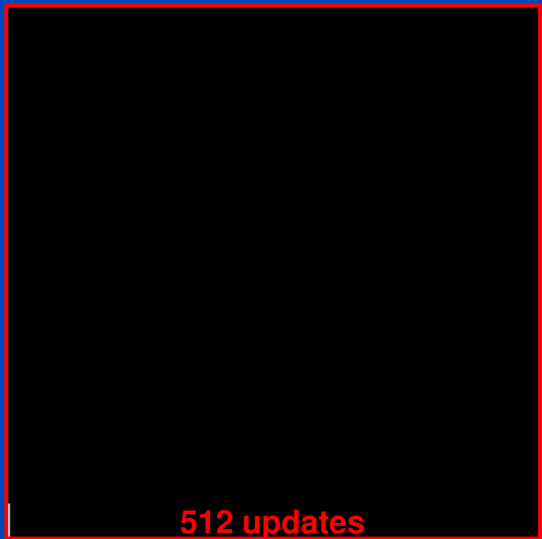

C = 0 HU, W = 1000 HU

Reconstructing Small FOVs

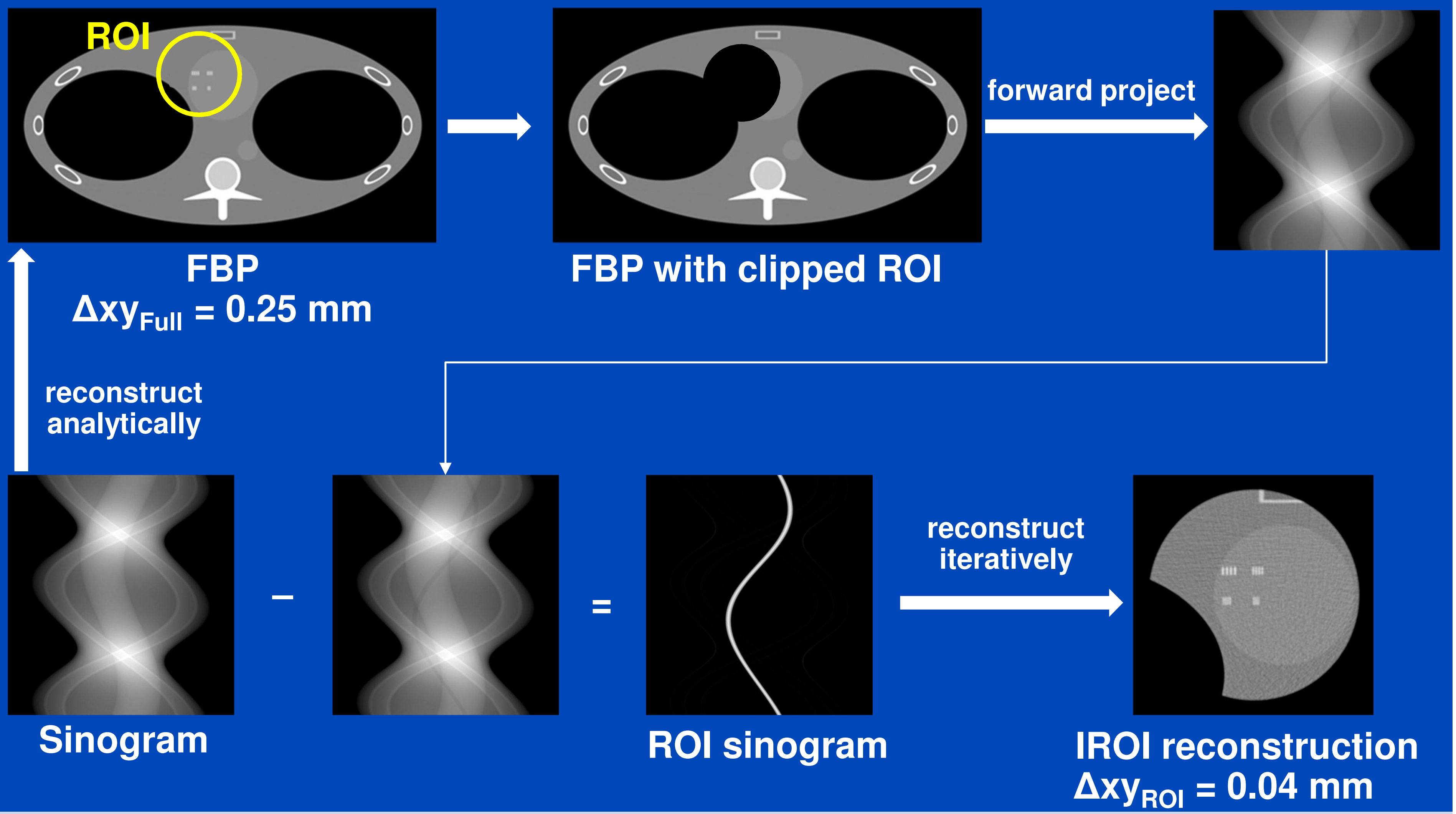

A. Ziegler, T. Nielsen, and M. Grass, “Iterative Reconstruction of Region of Interest for Transmission Tomography”, Med. Phys. 35 (4), Mar. 2008

Iterative != Iterative

- **In many cases artifact correction is iterative**
  - Higher order beam hardening correction
  - Cone-beam artifact correction
  - Scatter correction
- **Practical “iterative reconstruction” approaches**
  - often use empirical solutions
  - combine iterative with analytical reconstruction
  - combine iterative or analytical reconstruction with image restoration

Phase-correlated Feldkamp

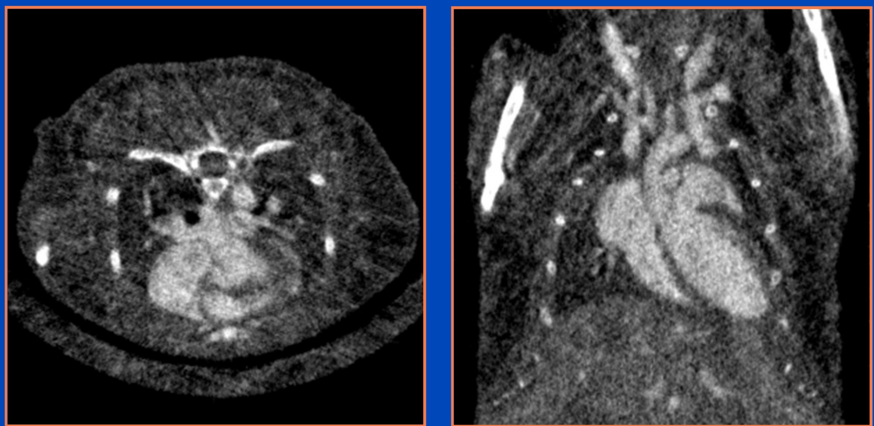

Low dose phase-correlated (LDPC) recon[1]

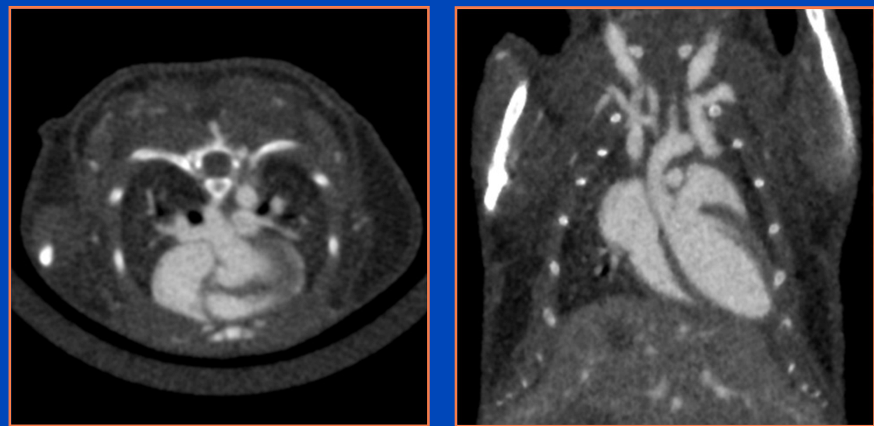

[1]S. Sawall, F. Bergner, R. Lapp, M. Mronz, A. Hess, and M. Kachelrieß, MedPhys 38(3), 2011

Iterative Reconstruction

- Aim: less artifacts, lower noise, lower dose
- Iterative reconstruction
  - Reconstruct an image.
  - Regularize the image.
  - Does the image correspond to the rawdata?
  - If not, reconstruct a correction image and continue.
- SPECT + PET are iterative for a long time!
- CT product implementations
  - AIDR (adaptive iterative dose reduction, Toshiba)
  - ASIR (adaptive statistical iterative reconstruction, GE)
  - iDose (Philips)
  - IMR (iterative model reconstruction, Philips)
  - IRIS (image reconstruction in image space, Siemens)
  - VEO, MBIR (model-based iterative reconstruction, GE)
  - SAFIRE, ADMIRE (advanced model-based iterative reconstruction, Siemens)

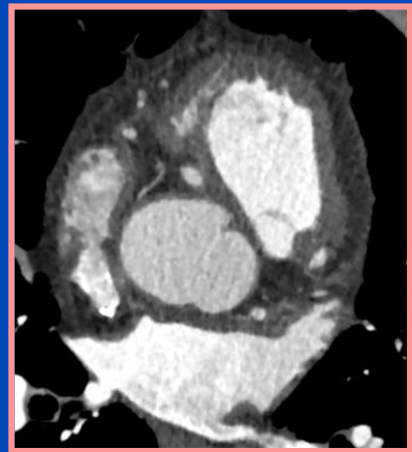

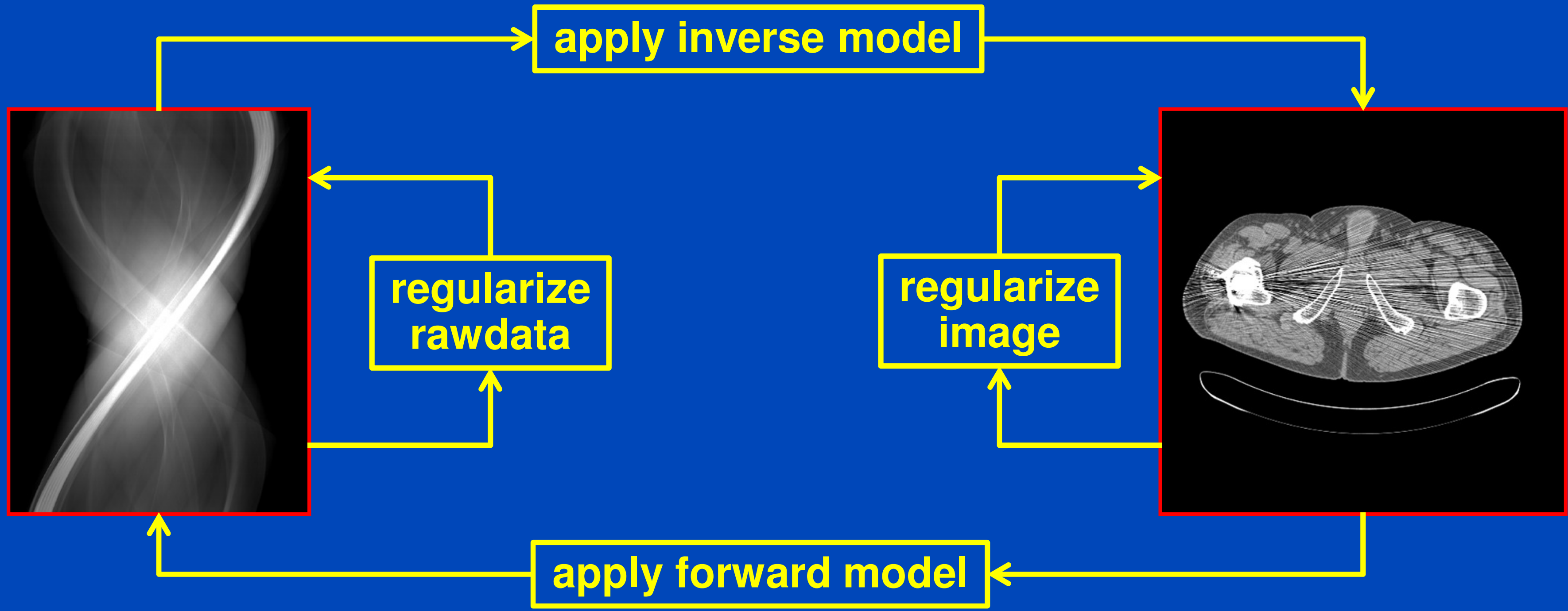

- Rawdata regularization: adaptive filtering[1], precorrections, filtering of update sinograms...
- Inverse model: backprojection (R^T) or filtered backprojection (R^{-1}). In clinical CT, where the data are of high fidelity and nearly complete, one would prefer filtered backprojection to increase convergence speed.
- Image regularization: edge-preserving filtering. It may model physical noise effects (amplitude, direction, correlations, …). It may reduce noise while preserving edges. It may include empirical corrections.
- Forward model (R_{phys}): Models physical effects. It can reduce beam hardening artifacts, scatter artifacts, cone-beam artifacts, noise, …

[1]M. Kachelrieß et al., Generalized Multi-Dimensional Adaptive Filtering, MedPhys 28(4), 2001

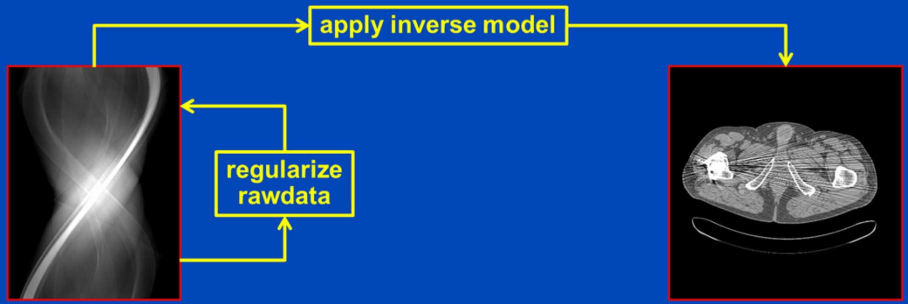

Conventional FBP with rawdata denoising (all vendors)

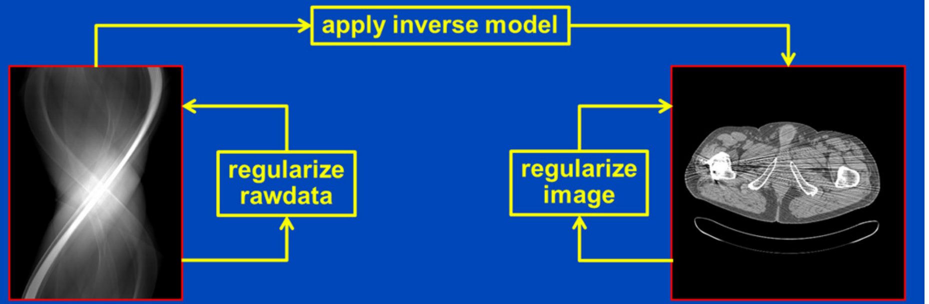

ASIR (Ge), AIDR3D (Toshiba), IRIS (Siemens), iDose (Philips)
SnapShot Freeze (GE), iTRIM (Siemens)

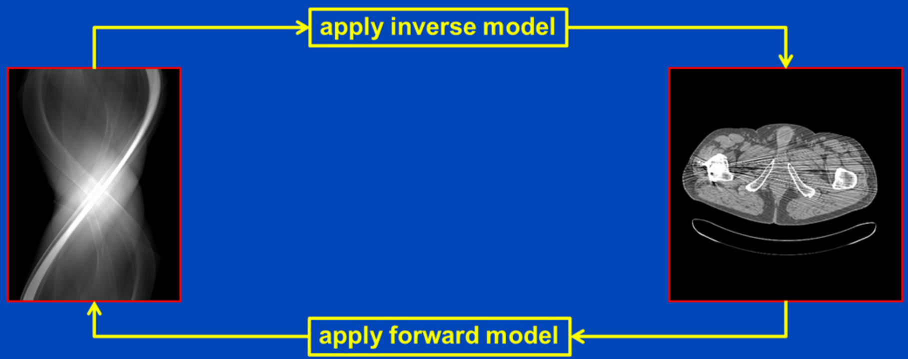

Veo/MBIR (Ge)

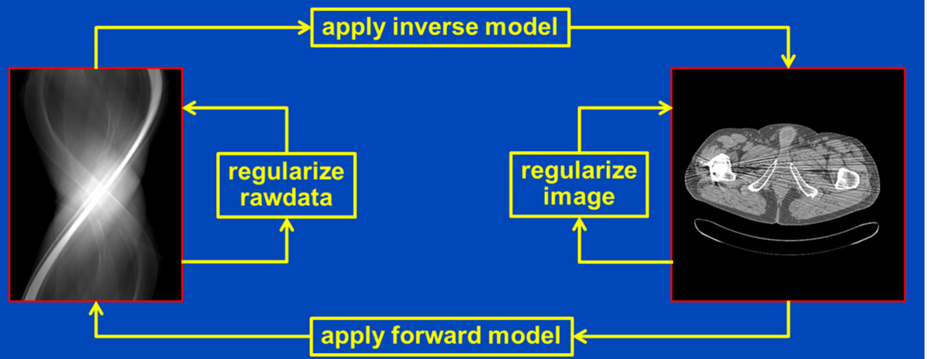

SAFIRE, ADMIRE (Siemens)

Plain FBP	Siemens Standard	IRIS VA34	SAFIRE VA40

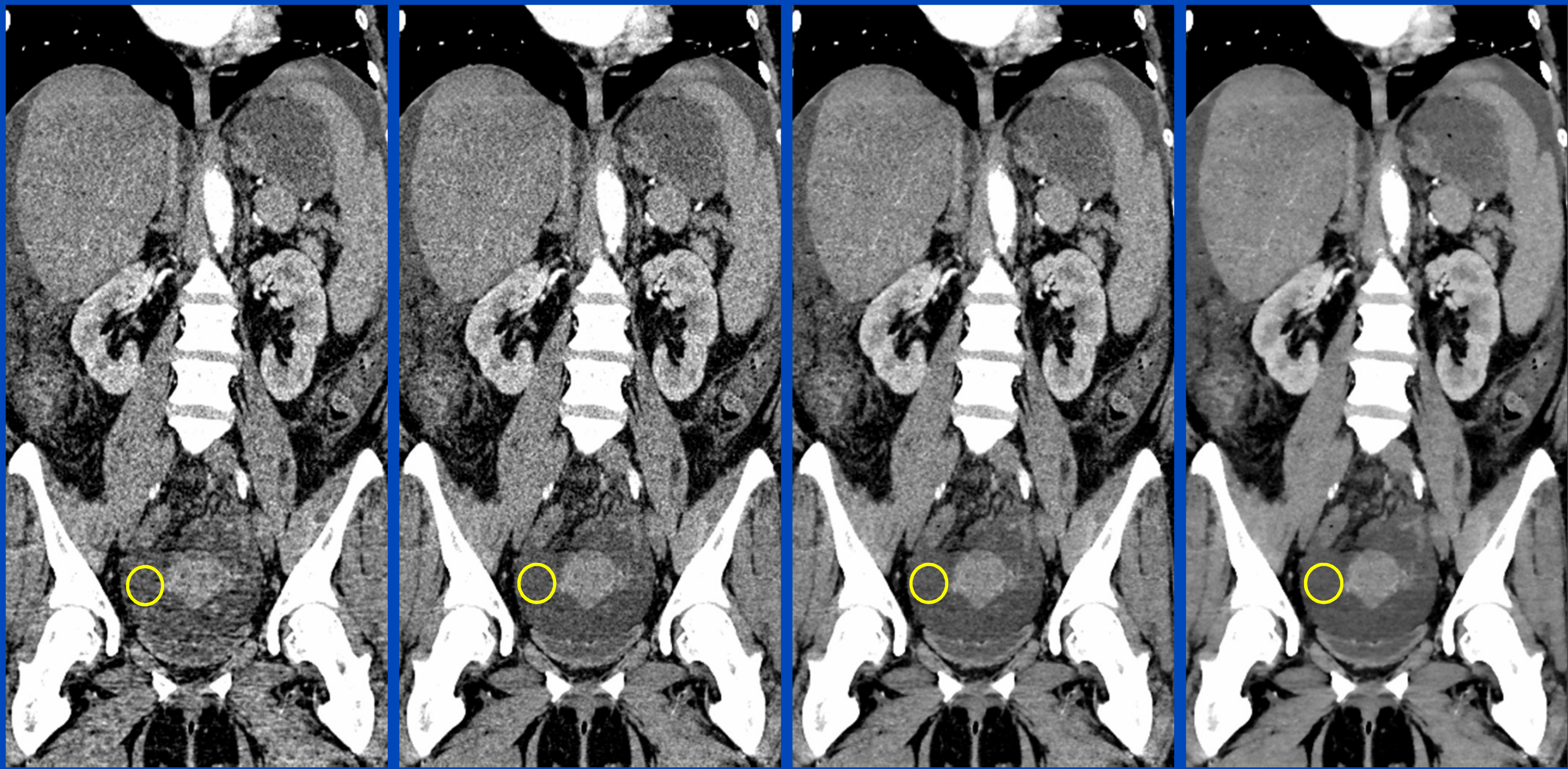

σ = 26.8 HU	σ = 17.6 HU	σ = 12.3 HU	σ = 7.8 HU

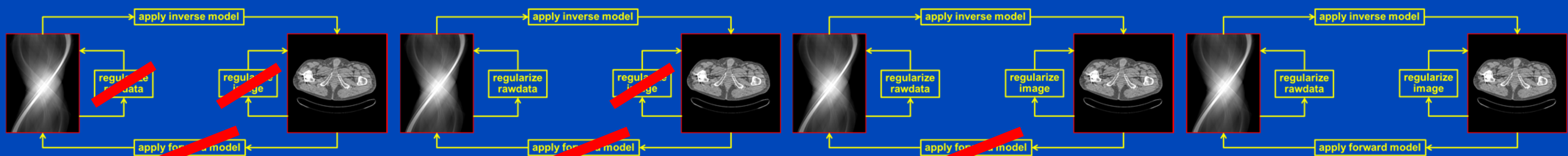

CT images provided by Siemens Healthcare, Forchheim, Germany

Courtesy of Dr. Jiang Hsieh, GE Healthcare Technologies, WI, USA.

Filtered Backprojection

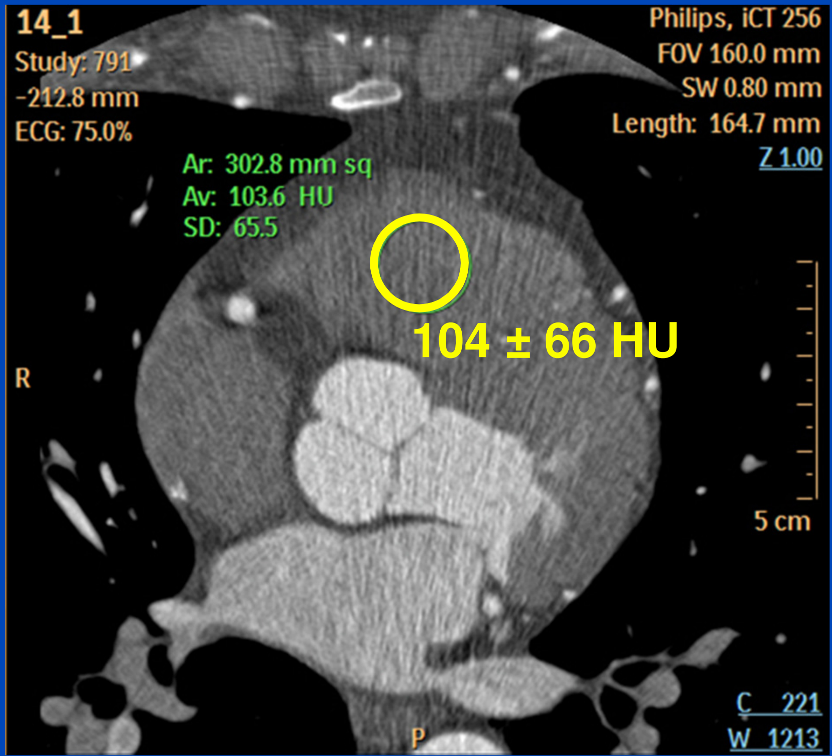

iDose 60%

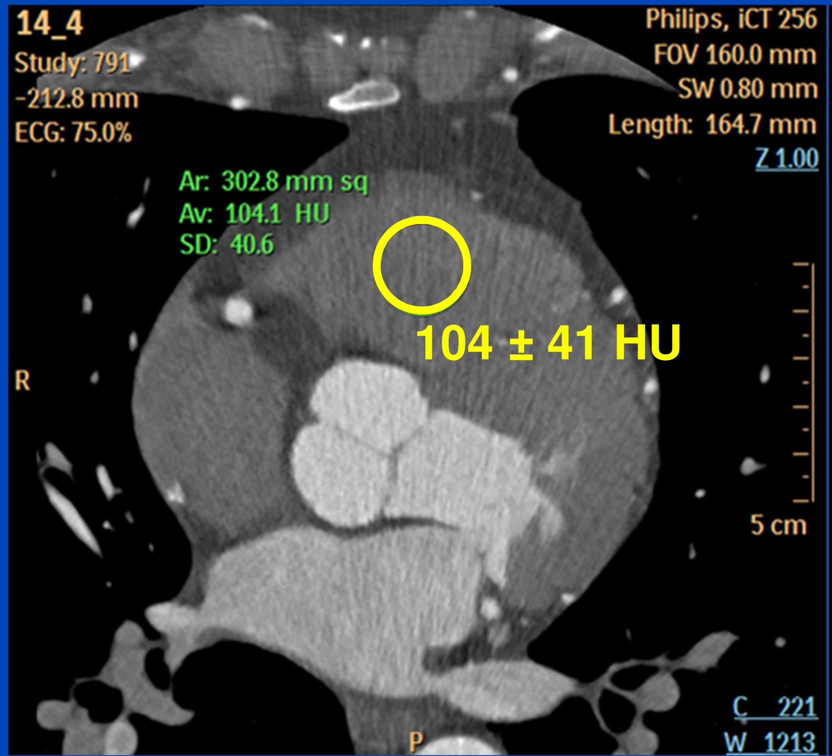

Courtesy of Dr. Waldemar Hosch, Zürich, Switzerland.

dkfz.

FBP

IMR

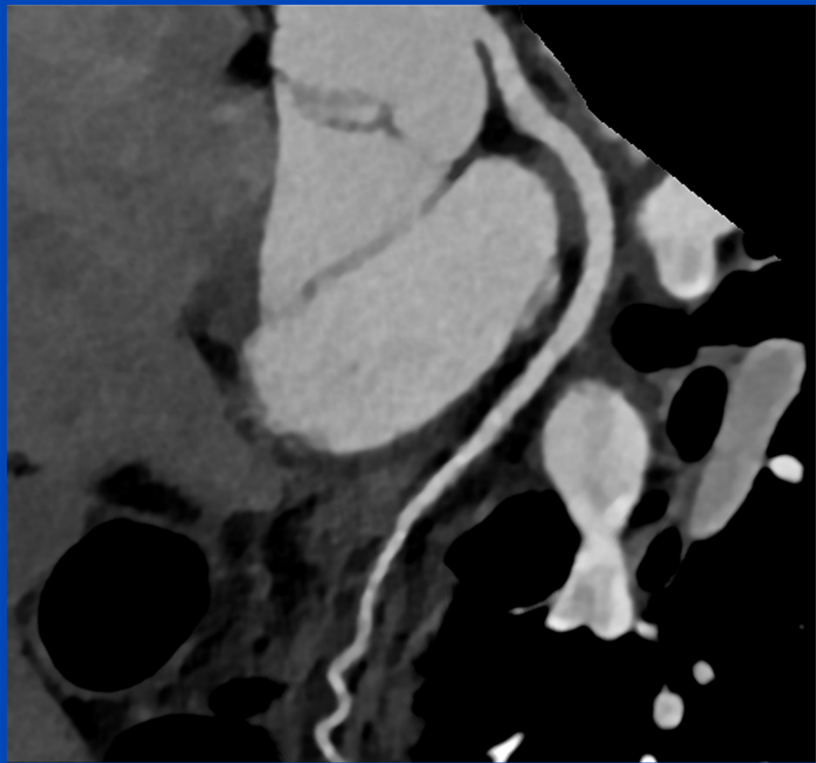

Courtesy of Dr. Thomas Köhler, Philips, Germany.

Filtered Backprojection | SAFIRE | SAFIRE

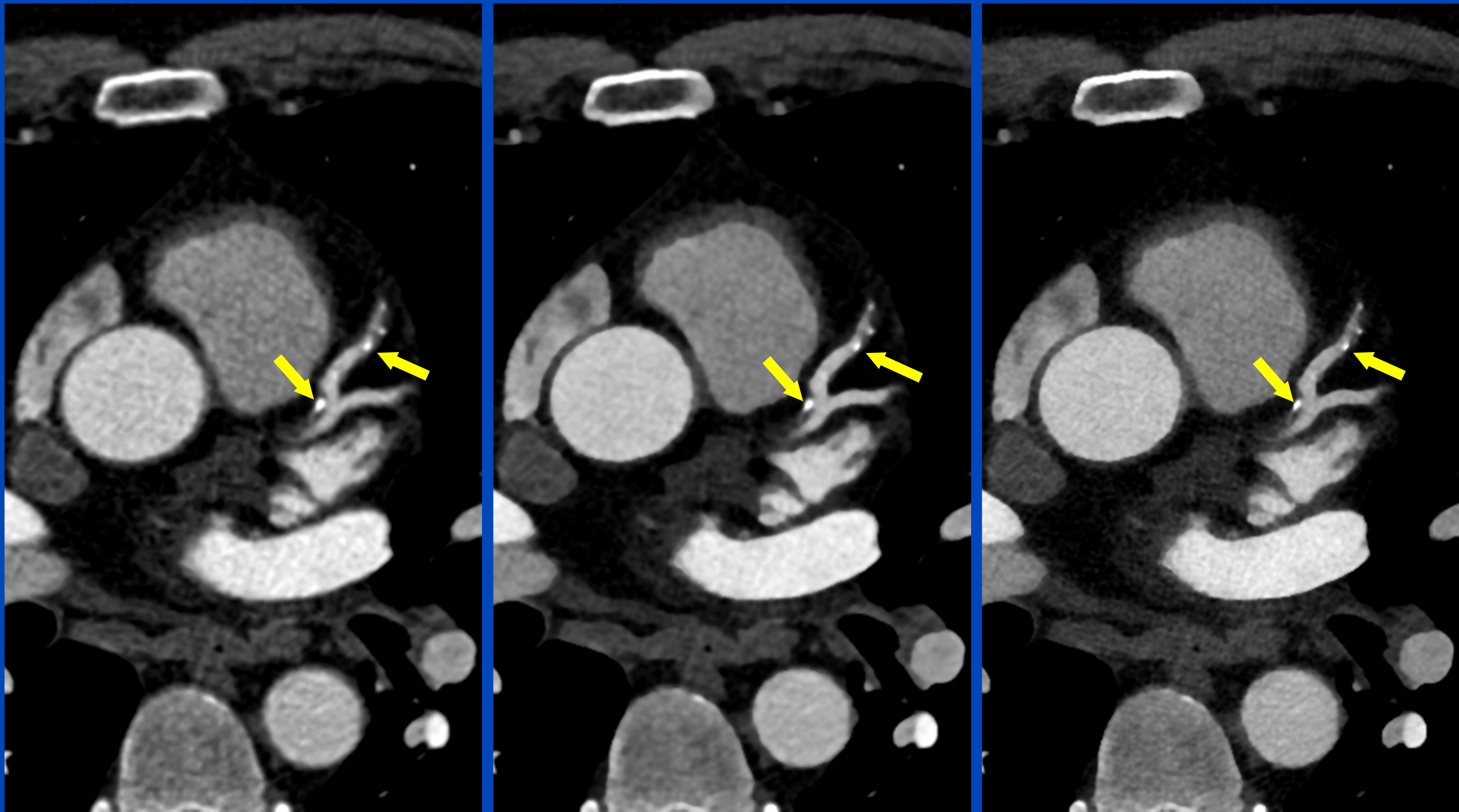

B26f | I26f strength 4 | I36f strength 4

Courtesy of Siemens Healthcare, Forchheim, Germany.

dkfz.

Filtered Backprojection

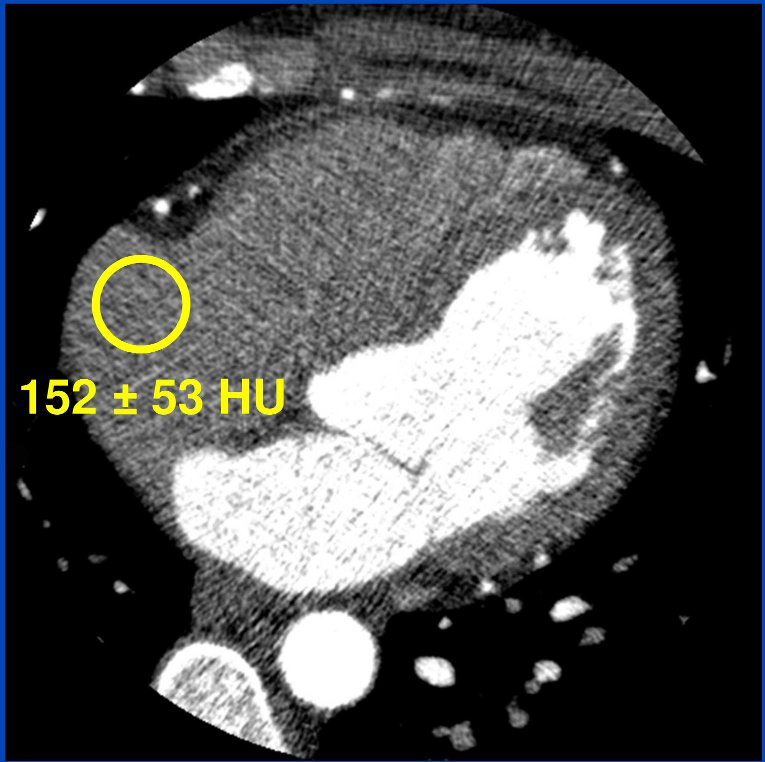

AIDR3D

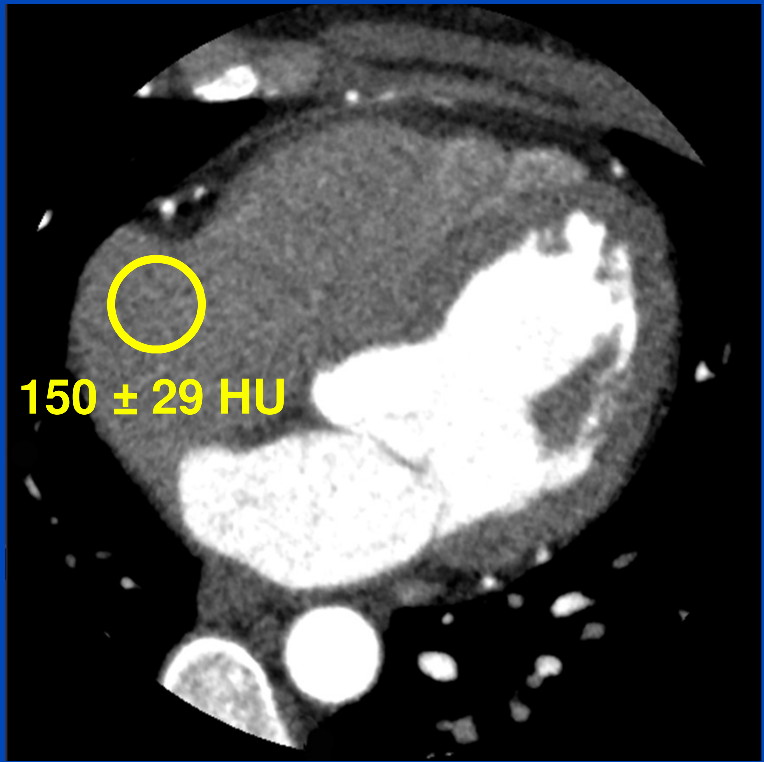

Filtered Backprojection

AIDR3D mild

AIDR3D standard

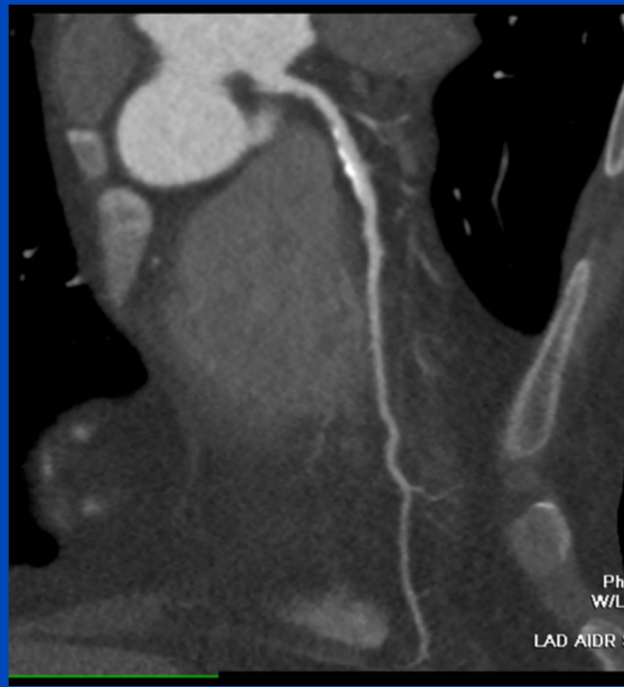

Courtesy of Dr. Patrik Rogalla, UHN, Toronto, Canada

SIEMENS

Advantages of SAFIRE versus Linear Noise Reduction

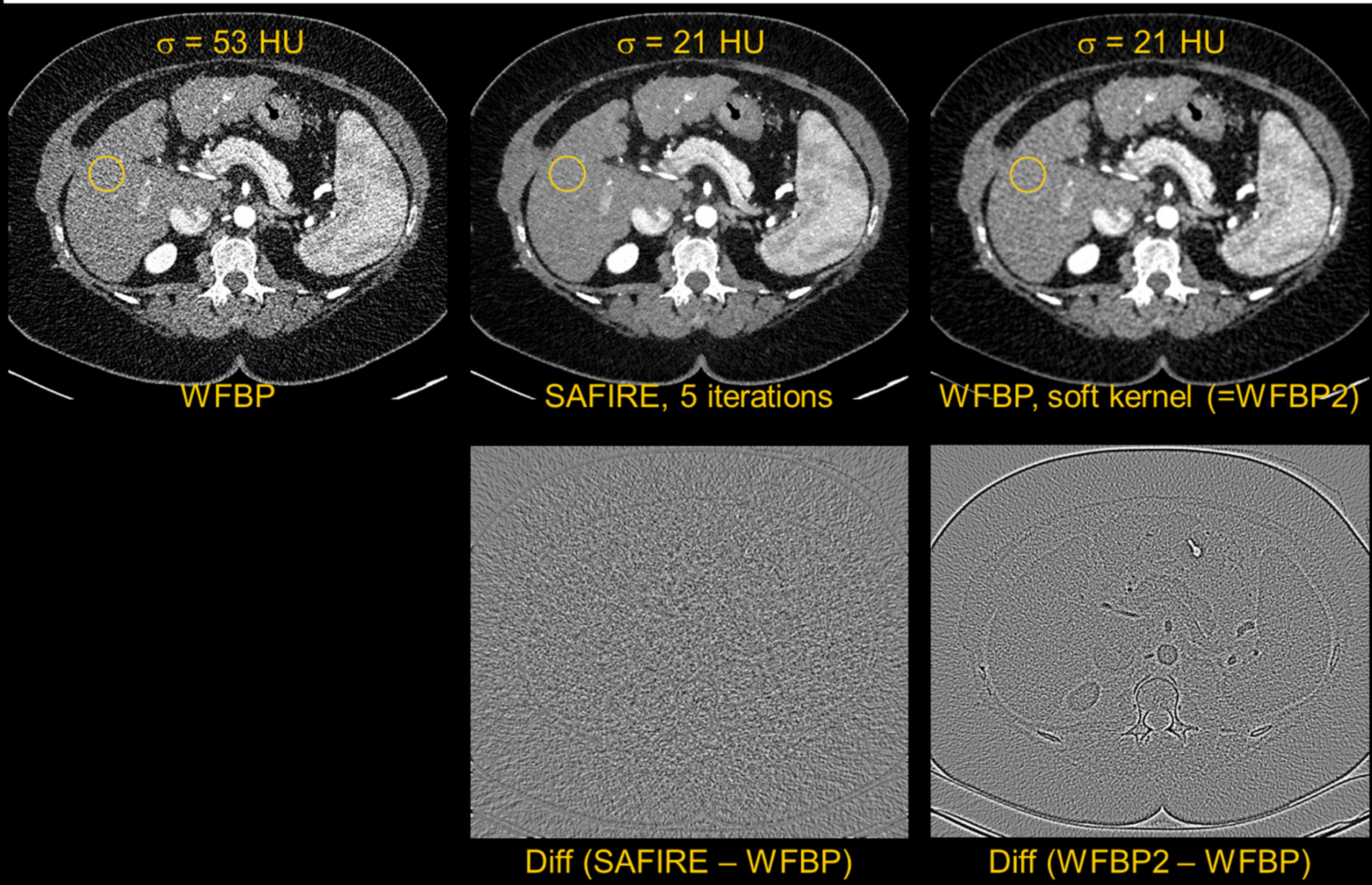

Figure provided by Siemens Healthcare, Forchheim, Germany

Conventional reconstruction

at 100% dose

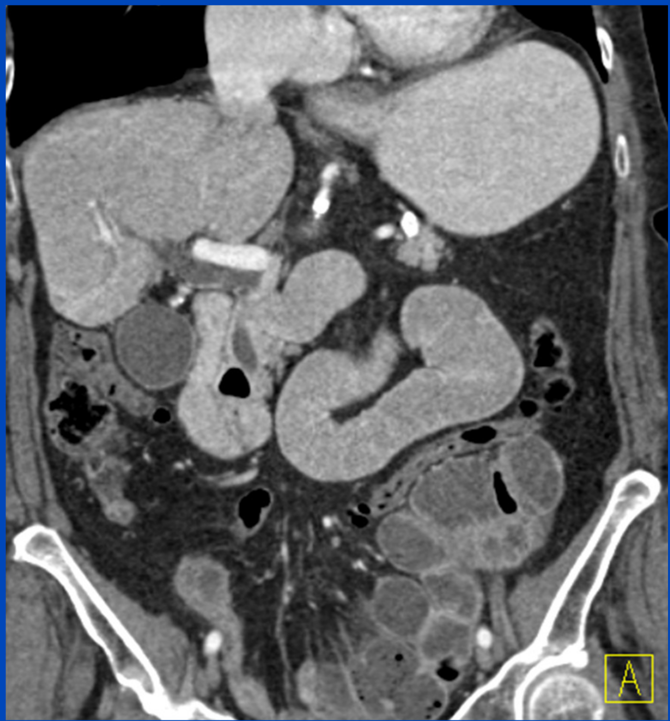

Iterative reconstruction and restoration

at 40% dose

Images provided by Siemens Healthcare, Forchheim, Germany

Conventional reconstruction

at 100% dose

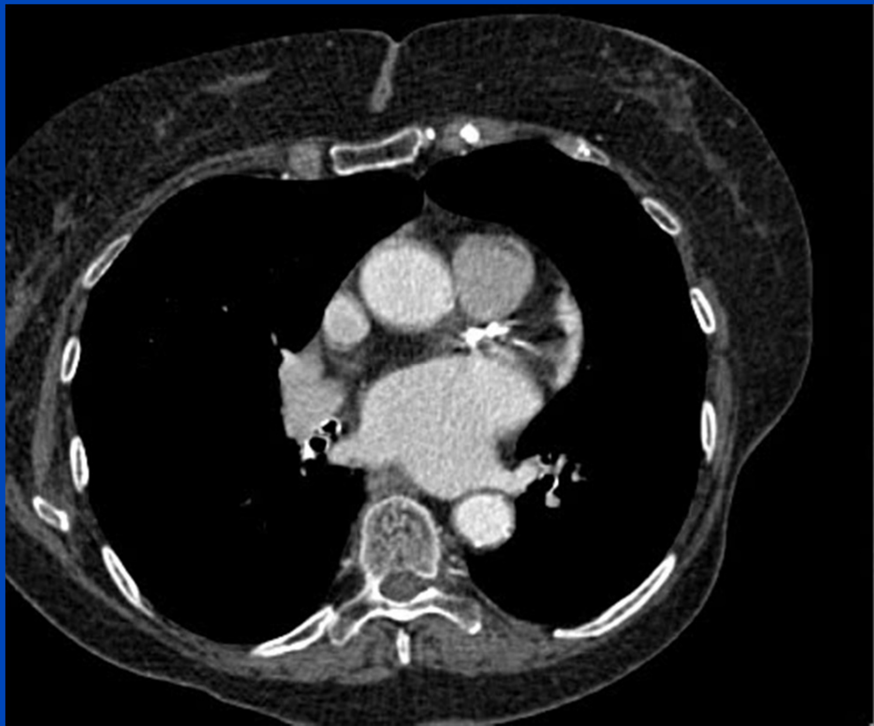

Iterative reconstruction and restoration

at 40% dose

Images provided by Siemens Healthcare, Forchheim, Germany

Conventional reconstruction

at 100% dose

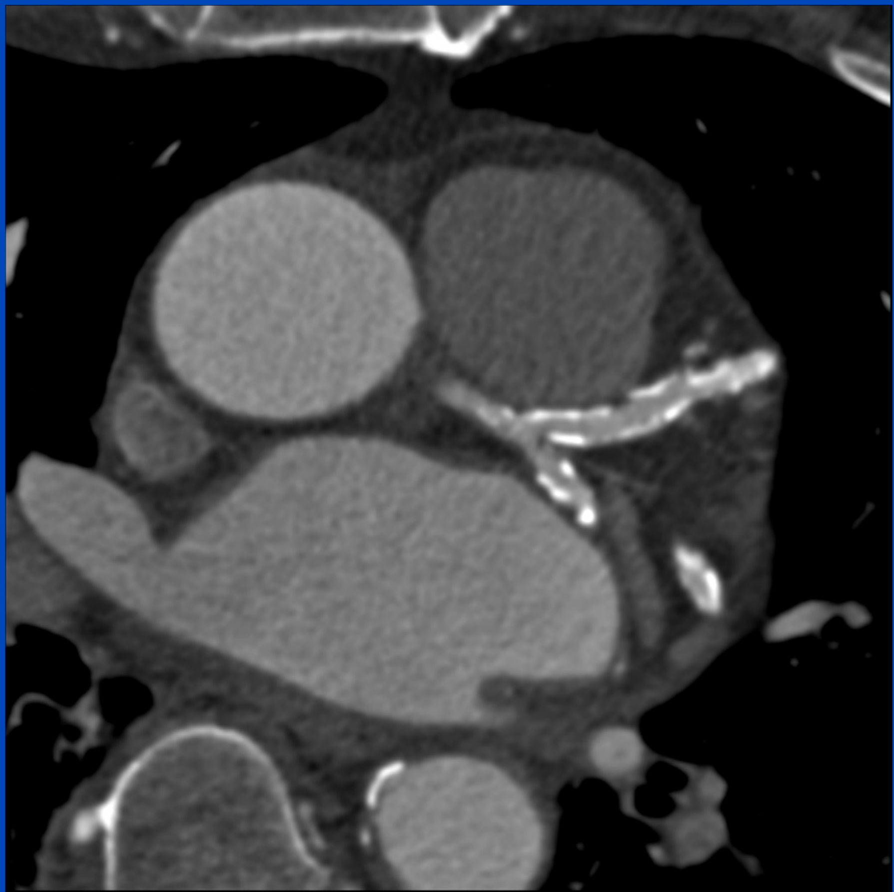

Iterative reconstruction and restoration

at 40% dose

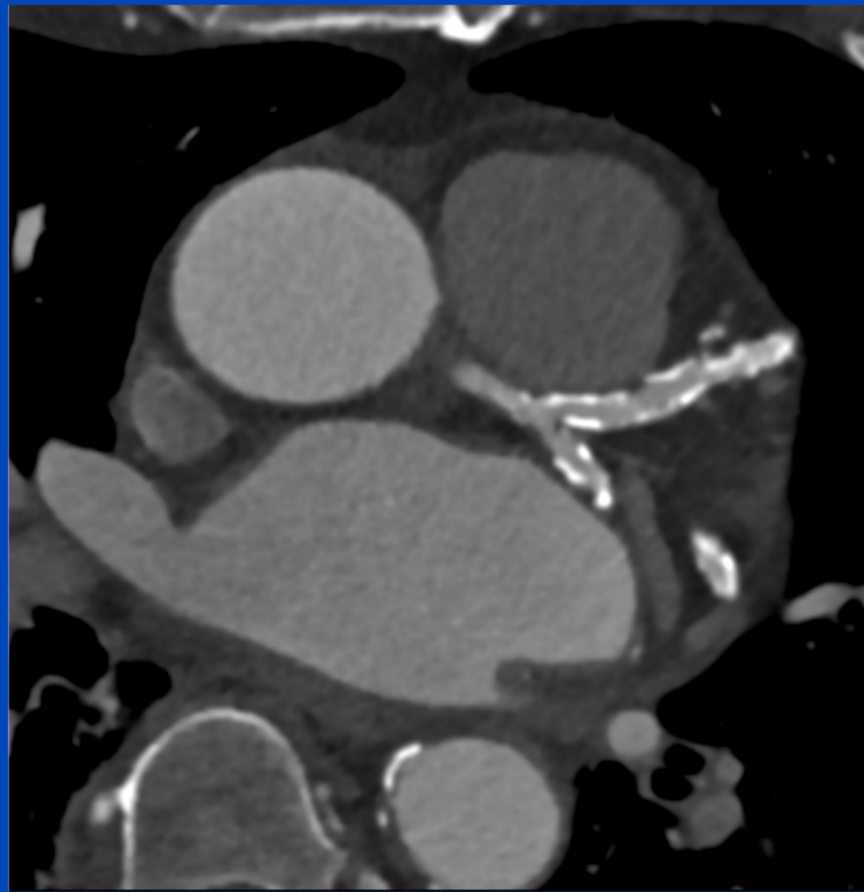

Images provided by Siemens Healthcare, Forchheim, Germany

dkfz.

Summary

- **Analytical image reconstruction**
  - is compute efficient
  - requires new solutions for new trajectories
  - is what most images are reconstructed with
- **Iterative image reconstruction**
  - requires much more computational effort
  - allows to easily model constraints
  - allows to incorporate prior knowledge
- **Practical modern solutions**
  - often are a combination of analytical and iterative recon
  - are offered by the major manufacturers of diagnostic CT

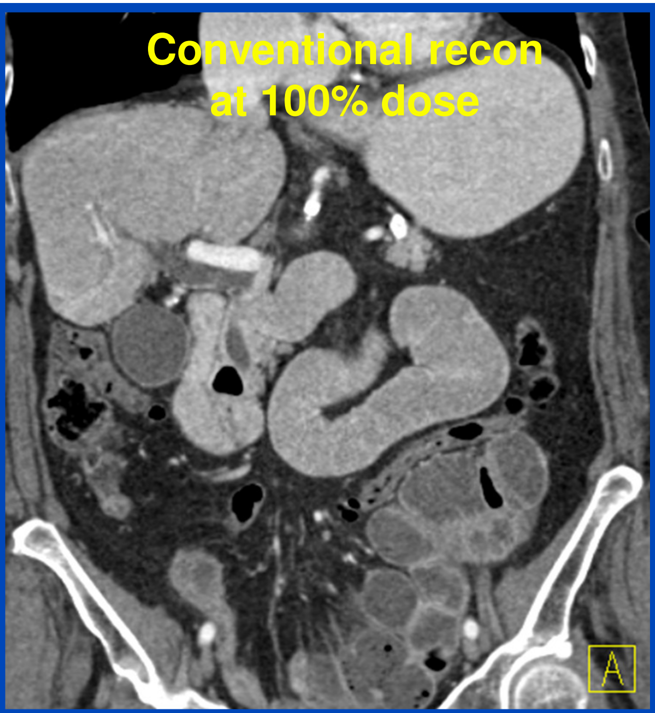

Images provided by Siemens Healthcare, Forchheim, Germany

Dose reduction values iterative compared to analytical image reconstruction claimed by clinical papers 2012 and earlier.

		GE		Philips		Siemens		Toshiba	
Type	Reference	ASIR	MBIR/Veo	iDose	IMR	IRIS	SAFIRE	AIDR	AIDR3D
Cardiac	[33]					38%*			
Cardiac	[36]						≥ 50%		
Cardiac	[37]						56%		
Cardiac	[29]			55%					
Cardiac	[25]	30%-45%*							
Cardiac	[20]	27%							
Cardiac	[38]						≥ 50%		
Cardiac	[34]					40%-51%			
Cardiac	[30]			52%*					
Cardiac	[35]					62%			
Cardiac	[45]							22%	
Cardiac	[39]						50%		
Cardiac	[46]								50%
Cardiac	[21]	23%	60%						
Cardiac	[22]	29%							
Cardiac	[23]	36%							
Cardiac	[28]			29%					
Abdominal/Chest	[79]	32%-65%							
Abdominal/Chest	[80]	15%*							
Abdominal/Chest	[81]			42%					
Abdominal/Chest	[82]	80%-90%							
Abdominal/Chest	[83]					36%*			
Abdominal/Chest	[77]	38%-46%							
Abdominal/Chest	[40]						≥ 50%		
Abdominal/Chest	[84]	≥30%							
Abdominal/Chest	[85]								64%
Abdominal/Chest	[86]	50%							
Abdominal/Chest	[87]							52%	
Abdominal/Chest	[88]	28%							
Abdominal/Chest	[24]	50%							
Abdominal/Chest	[89]					35%			
Abdominal/Chest	[90]			20%-80%*					
Abdominal/Chest	[91]	23%-66%							
Abdominal/Chest	[92]					40%			
Abdominal/Chest	[93]					50%			
Abdominal/Chest	[94]					50%			
Abdominal/Chest	[95]	34%							
Abdominal/Chest	[96]	41%							
Abdominal/Chest	[97]	25%							
Abdominal/Chest	[98]	38%							
Abdominal/Chest	[27]		75%						
Head	[99]					20%			
Head	[100]					60%			
Head	[101]	31%							
Head	[102]	26%							
REVIEW (Cardiac)	[17]	40%-50%	60%-70%				40%-50%		
REVIEW (General)	[16]	23%-76%		50%-76%		20%-60%	50%		52%
REVIEW (Cardiac)	[18]	40%		30%-40%					

M. Kachelrieß, Current Cardiovascular Imaging Reports 6:268–281, 2013.

dkfz.

Take Home Messages

- Rebinning converts the fan-beam data to parallel beam.
- FBP is an analytical image reconstruction algorithm.
- FBP is the standard CT reconstruction algorithm.
- Spiral data often require z-interpolation followed by FBP.
- The spiral pitch value is defined as $p = d\,/\,M{\cdot}S$.
- Iterative reconstruction promises less noise and artifacts.
- Iterative reconstruction starts to replace FBP, however it is much more computational demanding.


Thank You!
This presentation will soon be available at www.dkfz.de/ct.
Parts of the reconstruction software were provided by RayConStruct® GmbH, Nürnberg, Germany.